Gravity with Gaia

Mariateresa Crosta
INAF
Astrophysical Observatory of Torino

XXIII SIGRAV Conference,
Urbino 7-9 Sept 2021

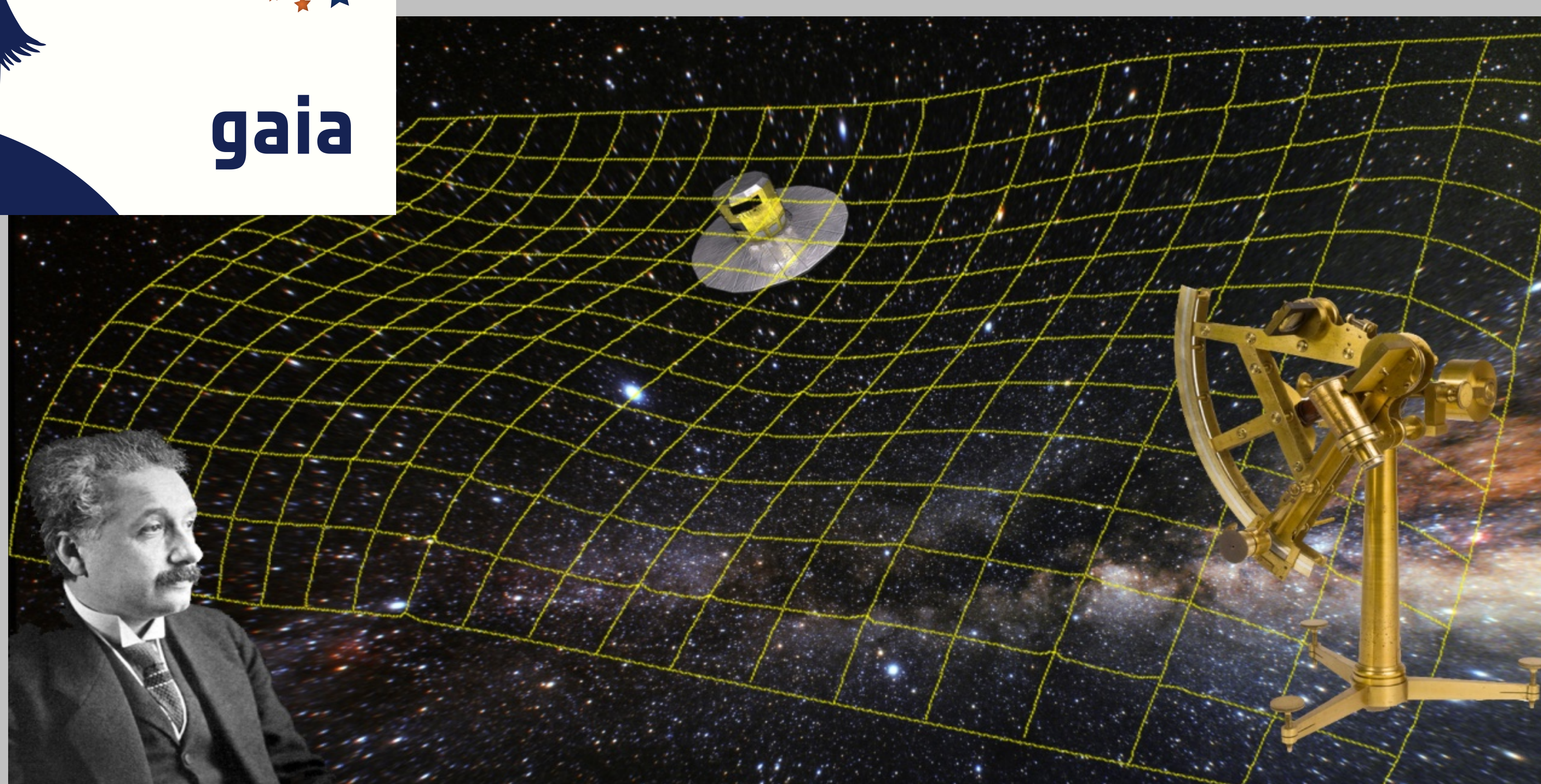

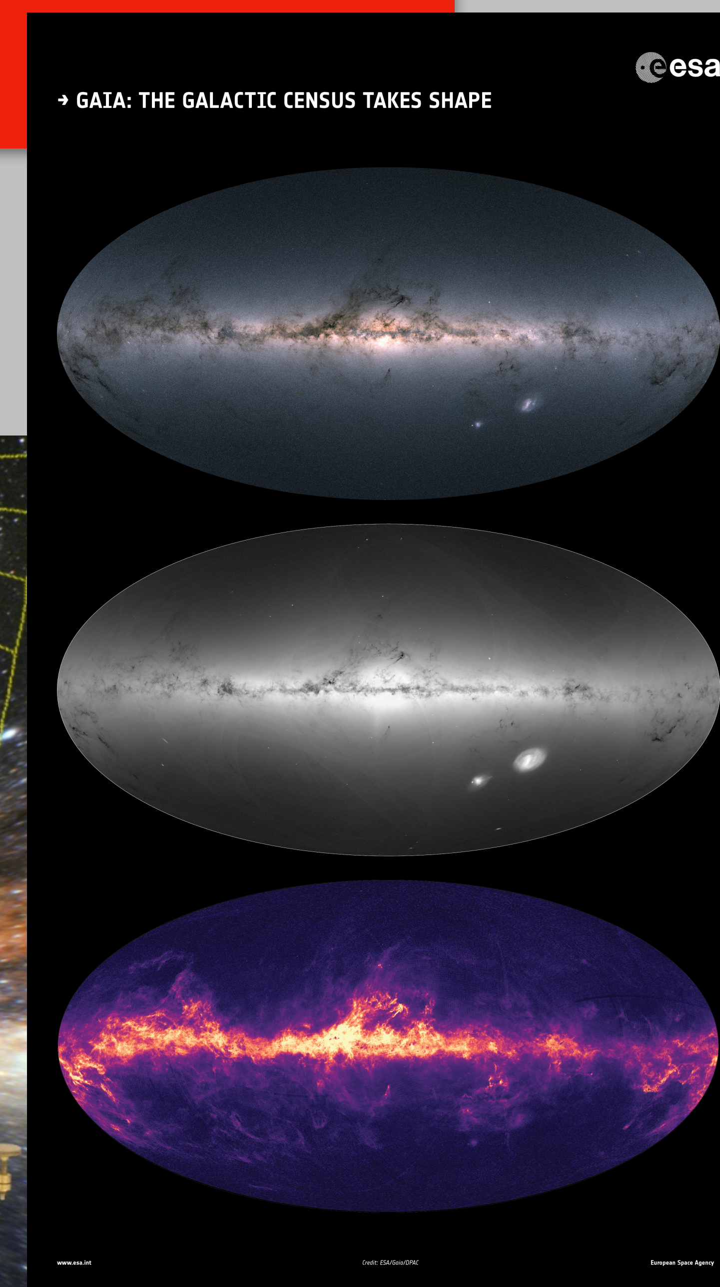

Outline

1. Why Gravity with Gaia

2. Relativistic Astrometry/Gravitational Astrometry

3. GR tests from Solar System to Milky Way scales

4. GW & relativistic astrometric observables from space

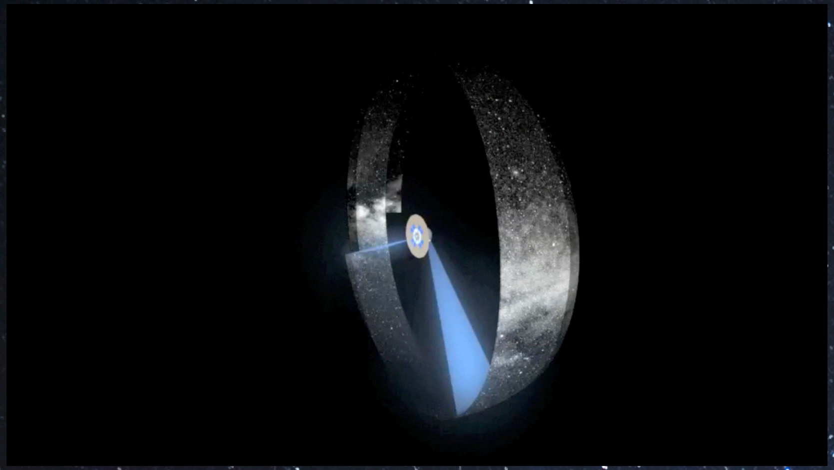

Gaia measures position (direction and distance)& velocity of over 1 billion stars in our Galaxy with an accuracy of up to 10 millionths-of-arcsecond

Science with one/two billion objects in 3 dimension, from structure and evolution of the MW to GR tests

Astrometry

positions
proper motions
parallaxes

end-of-mission astrometric accuracies better than 5-10µas (brighter stars)
130-600µas (faint targets)

Photometry

spectral classification
photometric distances
brightness
temperature
mass
age
chemical composition

G < 20.7 mag

Spectrometry

radial velocity
chemical abundances

G_RVS= 16.2

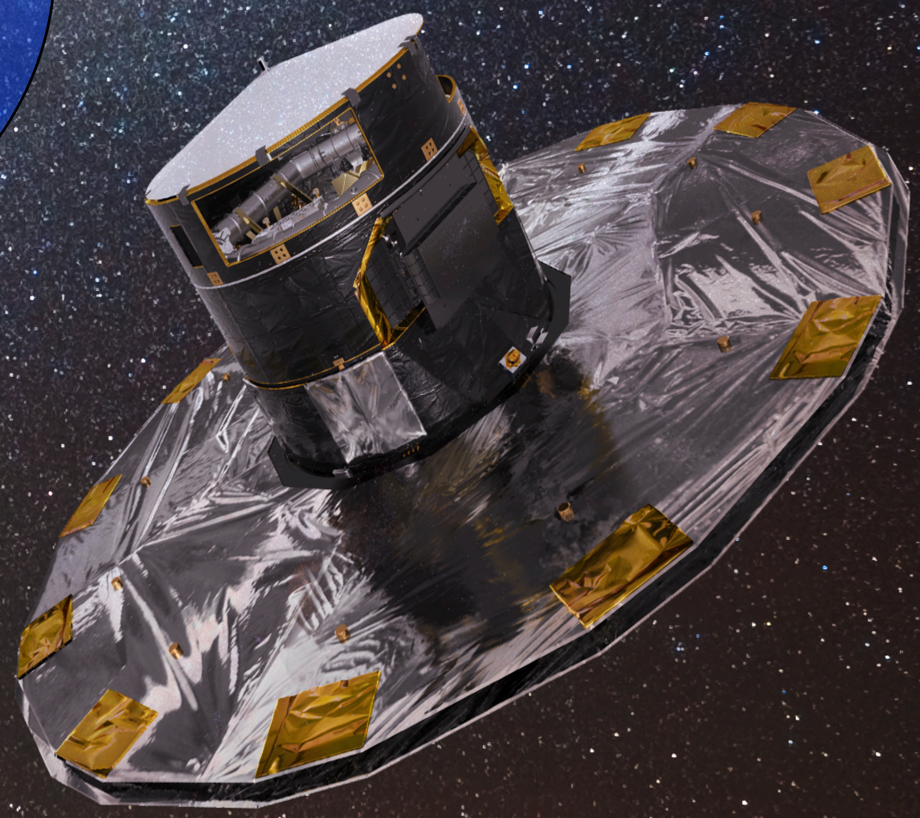

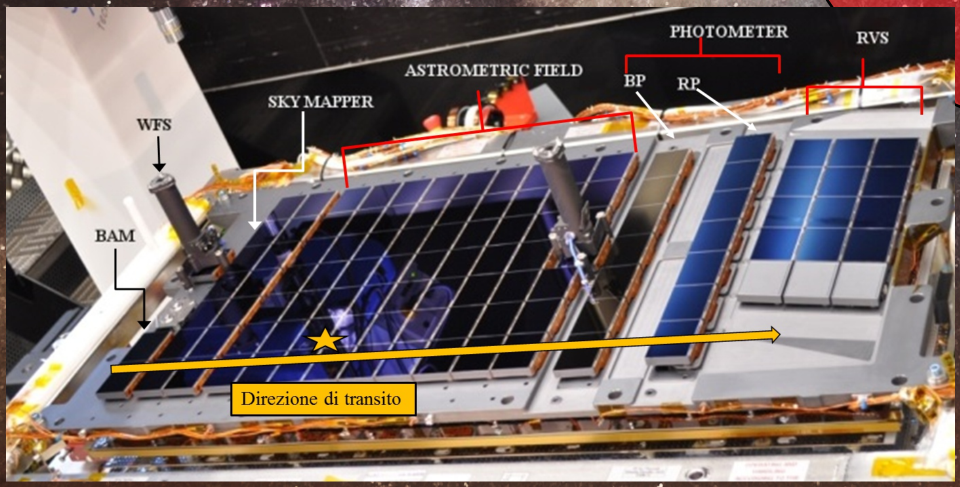

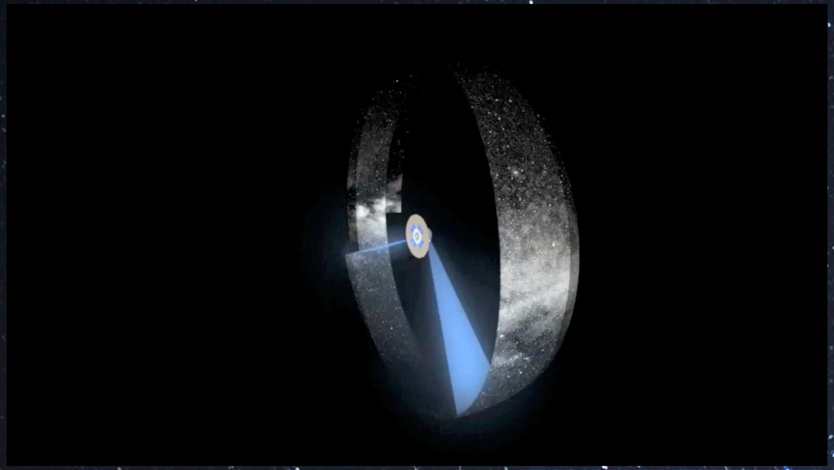

Gaia measures position (direction and distance)& velocity of over 1 billion stars in our Galaxy with an accuracy of up to 10 millionths-of-arcsecond

Science with one/two billion objects in 3 dimension, from structure and evolution of the MW to GR tests

Astrometry

positions
proper motions
parallaxes

end-of-mission astrometric accuracies better than 5-10µas (brighter stars)
130-600µas (faint targets)

Photometry

spectral classification
photometric distances
brightness
temperature
mass
age
chemical composition

G < 20.7 mag

Spectrometry

radial velocity
chemical abundances

G_RVS= 16.2

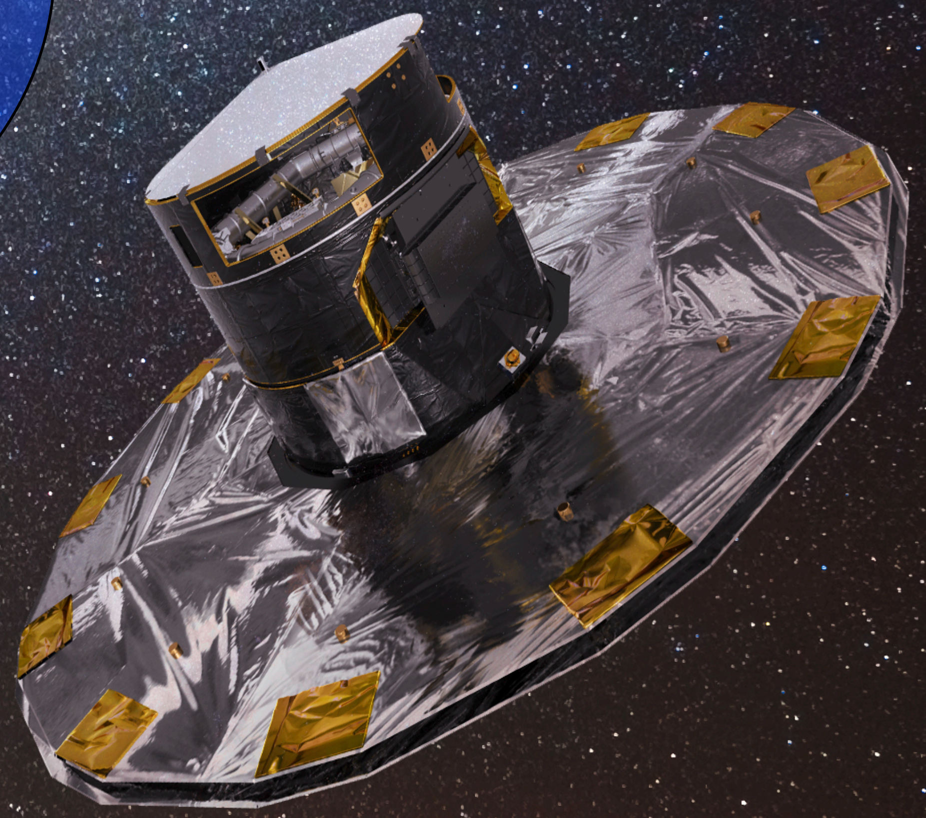

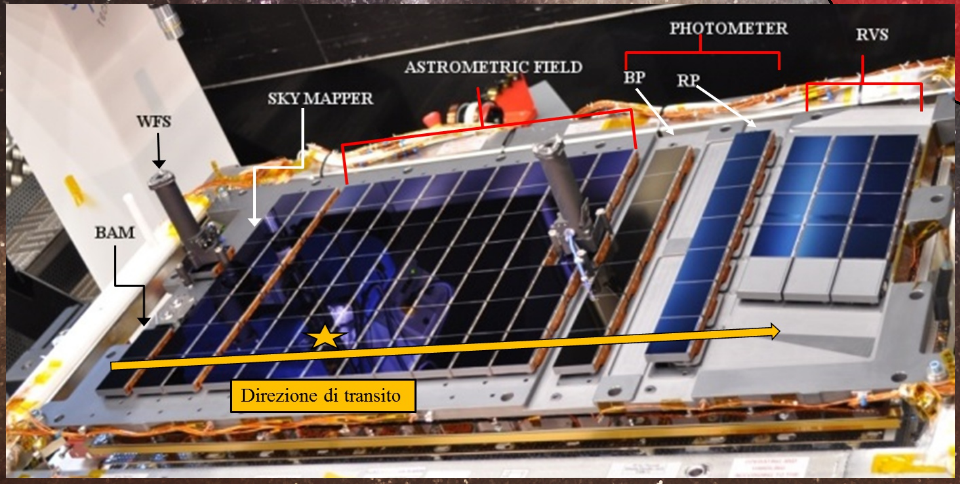

Relativistic Astrometry

1 microarcsecond

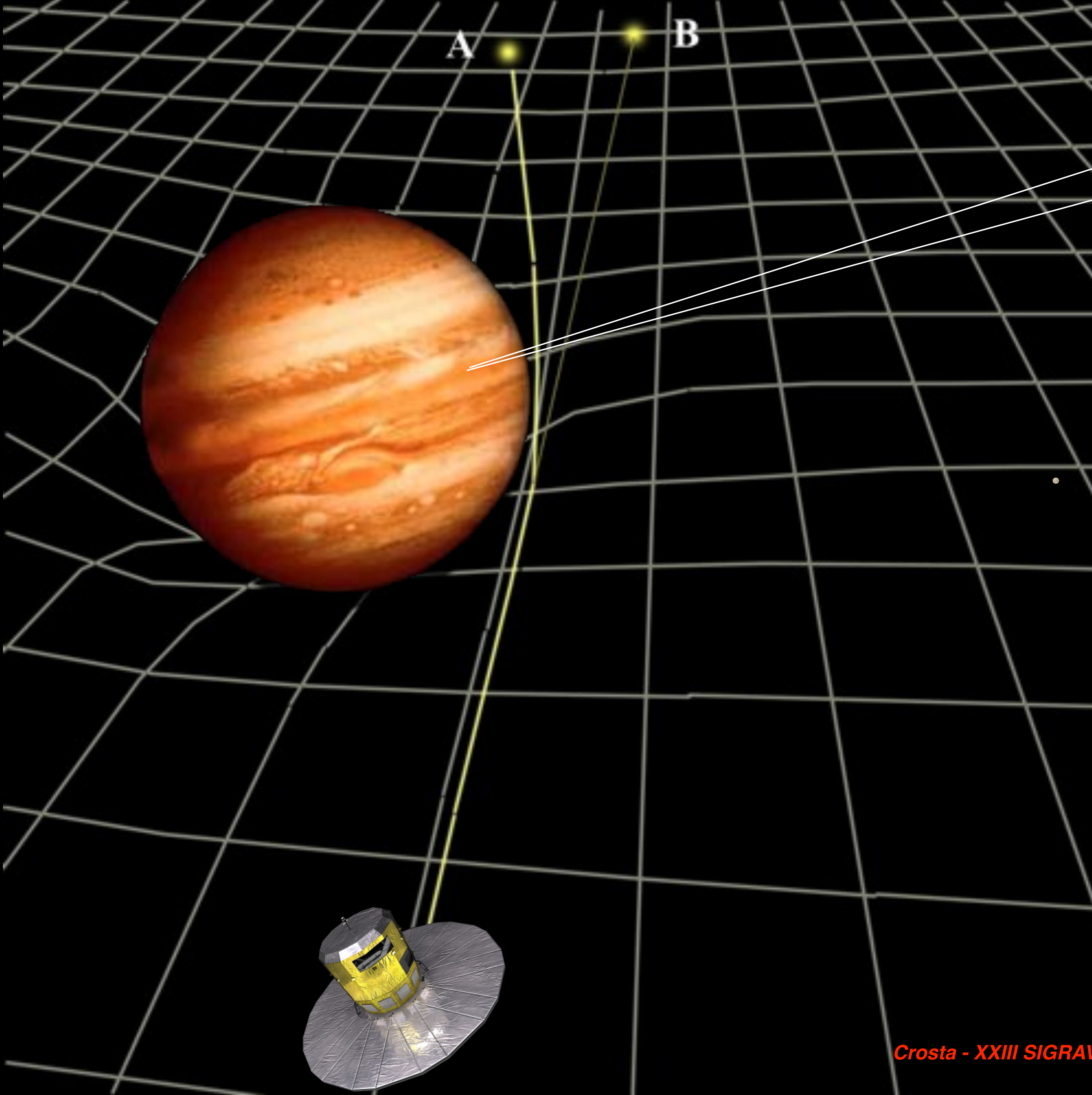

The location of an object in astrometry is considered reliable if its relative error is less 10%

parallax $\pi(\text{arcsec}) \approx 1(\text{UA})/\text{d*}(\text{pc})$

$$\pi \approx \sigma_\pi \cdot 10$$

Hipparcos	Gaia
$\sigma_\pi = 1\ \text{mas}$	$\sigma_\pi = 10\ \mu\text{as}$
↓	↓
$\pi \approx 10^{-2}\text{arsec}$	$\pi \approx 10^{-4}\text{arsec}$
↓	↓
d* = 100 pc	d*= 10 kpc

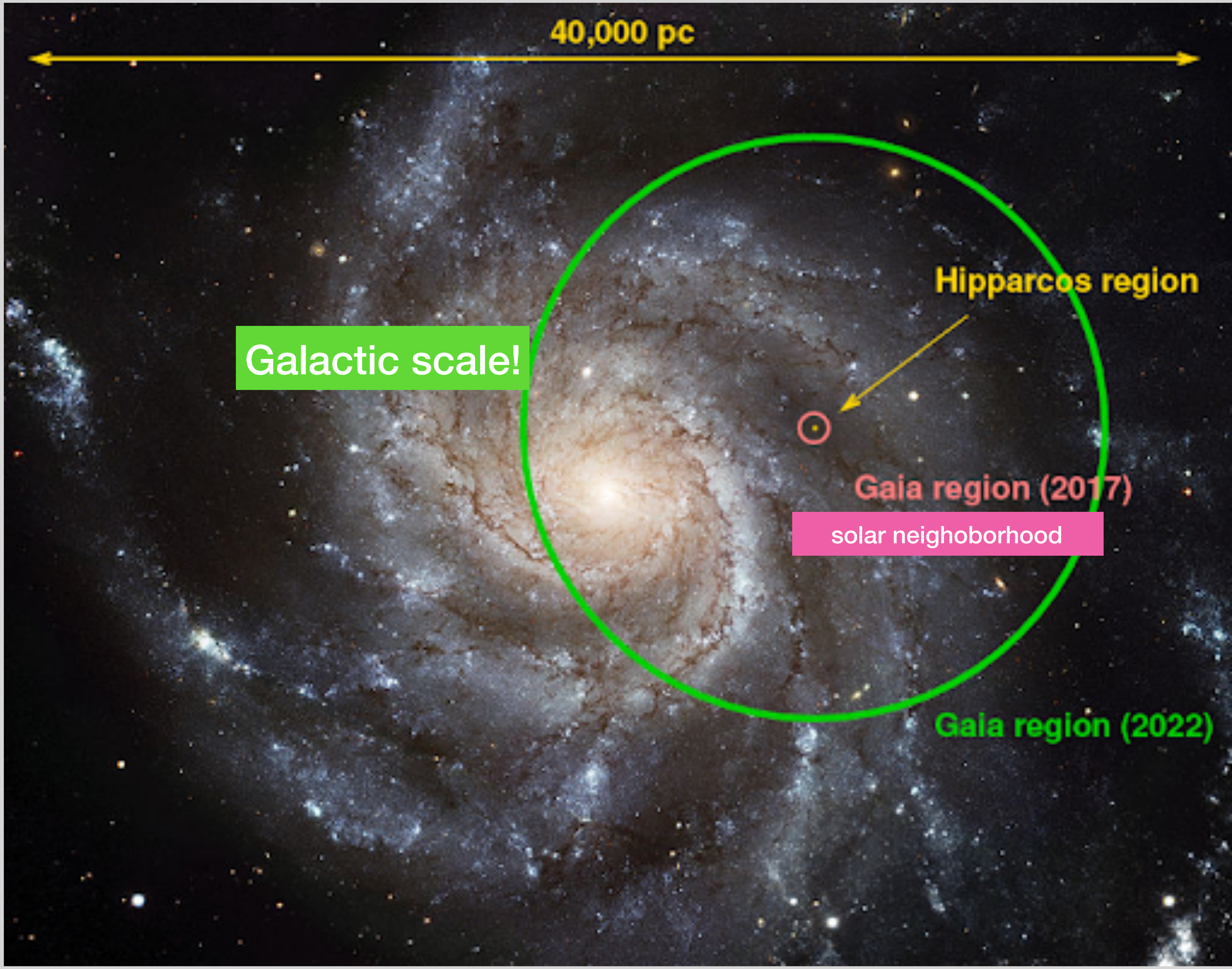

Gaia EDR3 - Milky Way

https://www.cosmos.esa.int/web/gaia/early-data-release-3

Gaia DR3 data (both Gaia EDR3 and the full Gaia DR3) are based on data collected between 25 July 2014 (10:30 UTC) and 28 May 2017 (08:44 UTC), **spanning a period of 34 months**.

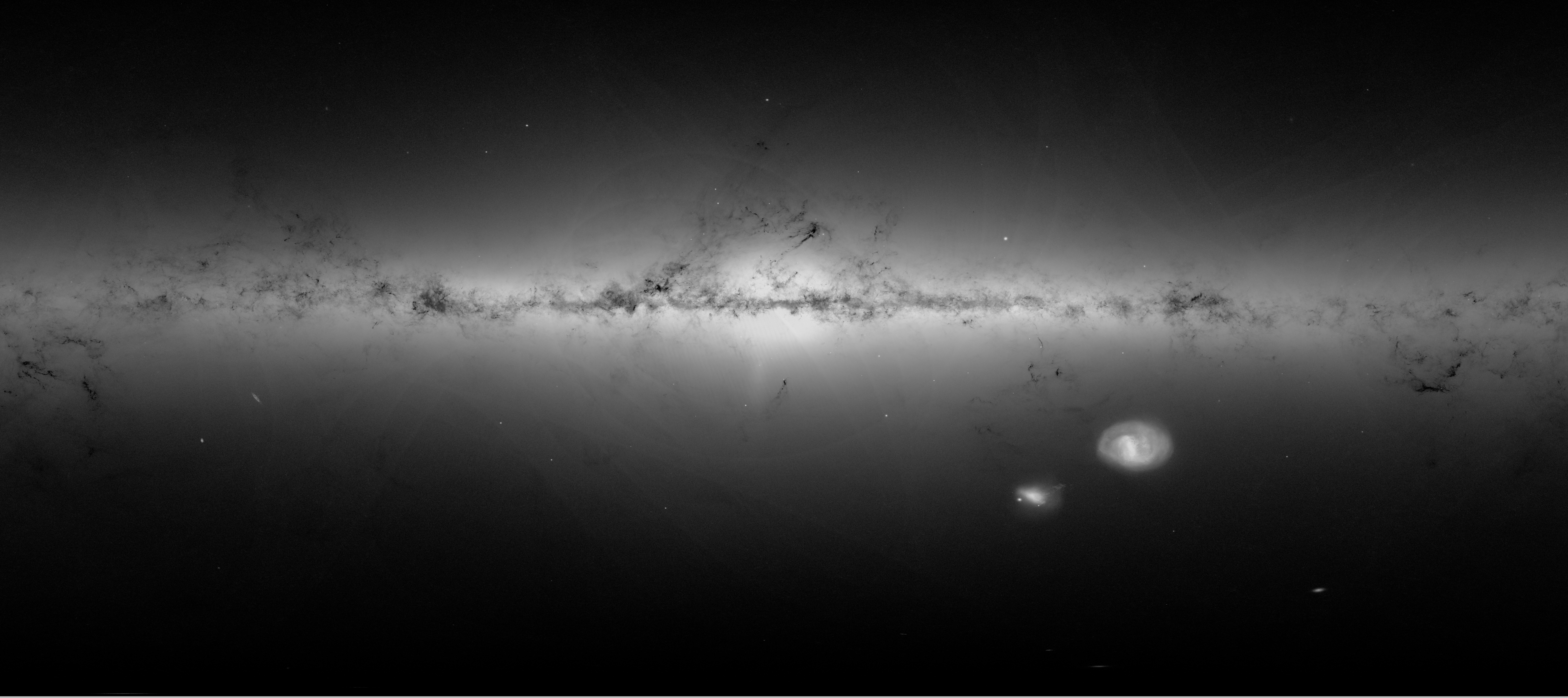

Source count maps based on the Gaia EDR3 data.
Image credit: ESA/Gaia/DPAC

Acknowledgement: Images were created by André Moitinho and Márcia Barros, University of Lisbon, Portugal

Gaia-observer laboratory the Solar System

micro-arcsecond accuracy+ dynamical gravitational fields
relativistic models of light propagation:
RELATIVISTIC ASTROMETRY

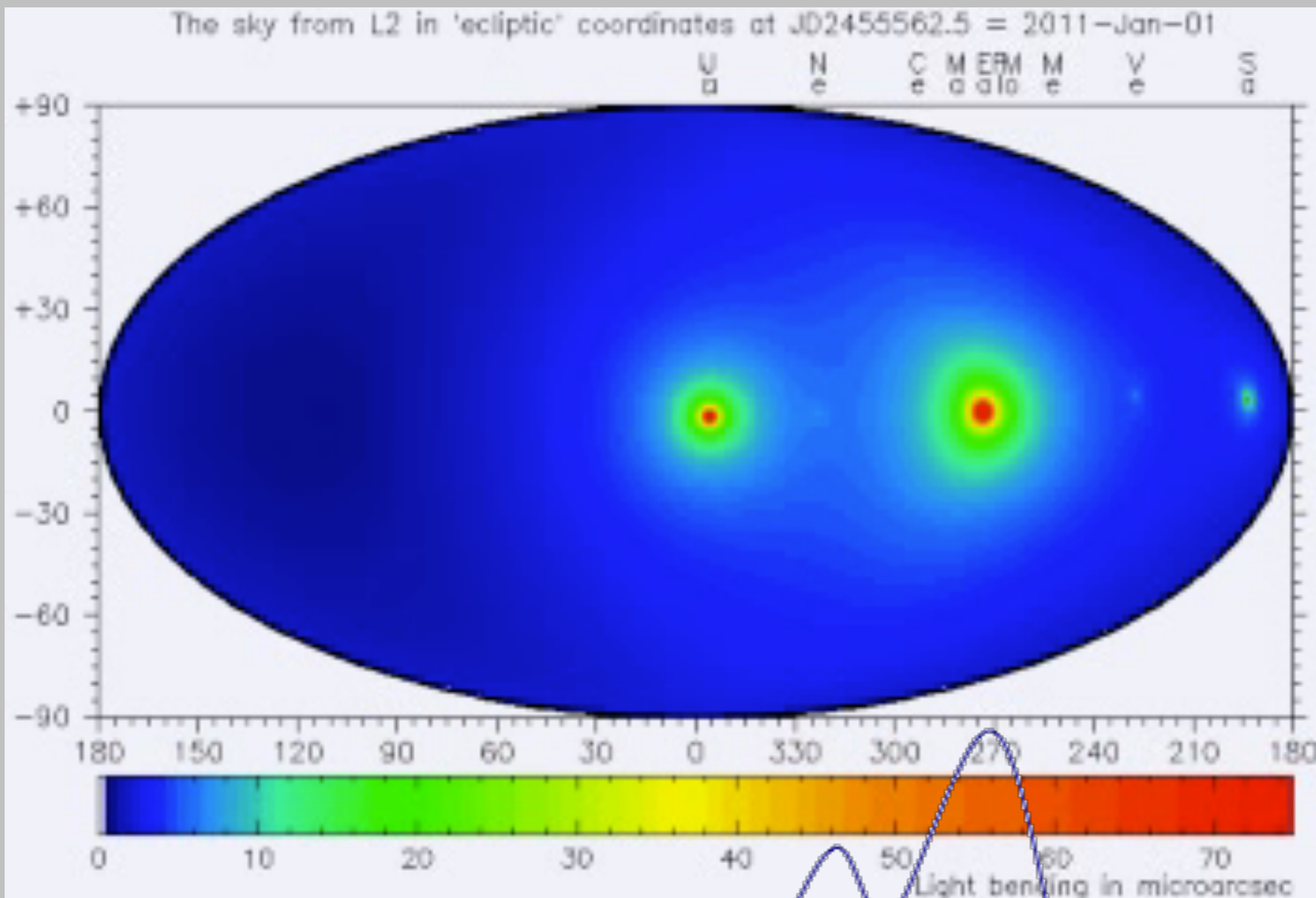

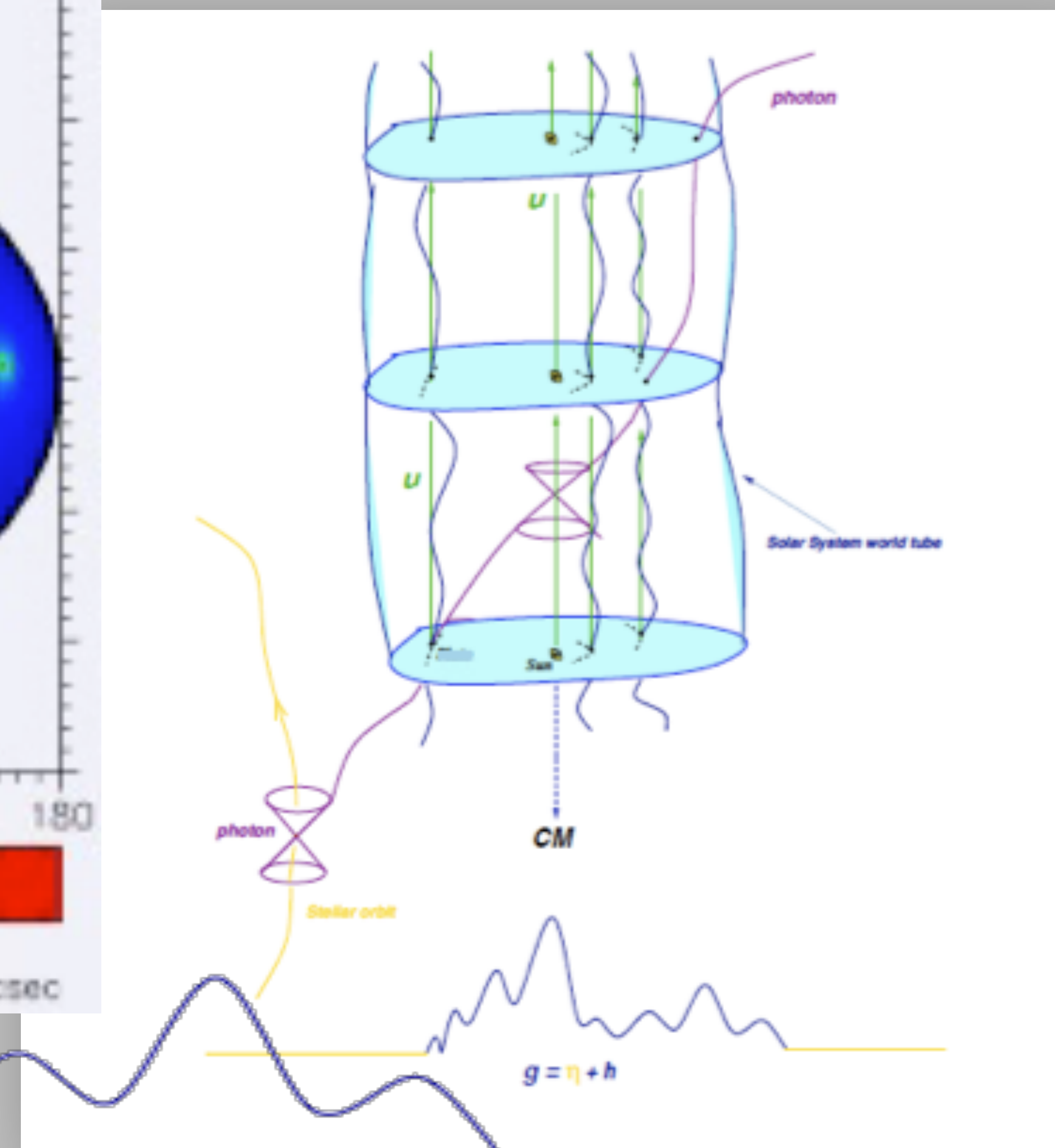

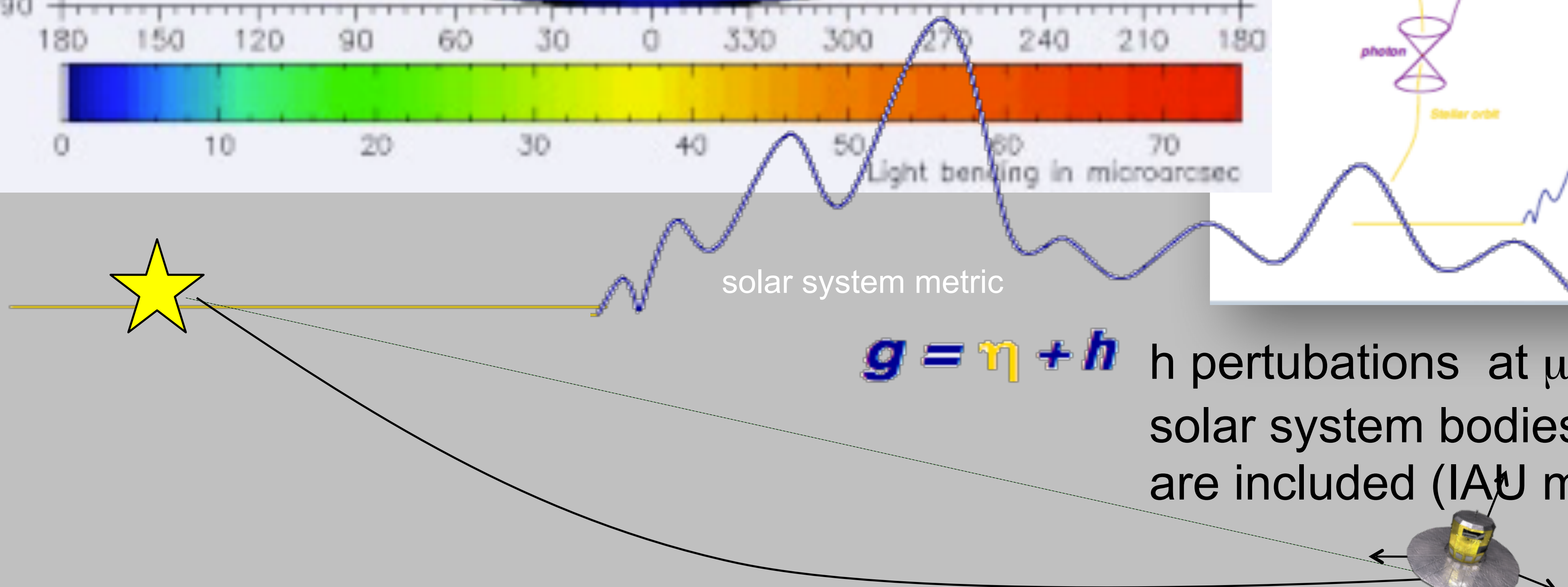

$g = \eta + h$ h pertubations at μ-**arcsec** due to the solar system bodies. Off-diagonal terms are included (IAU metric)

Gaia-observer laboratory the Solar System

micro-arcsecond accuracy+ dynamical gravitational fields
relativistic models of light propagation:
RELATIVISTIC ASTROMETRY

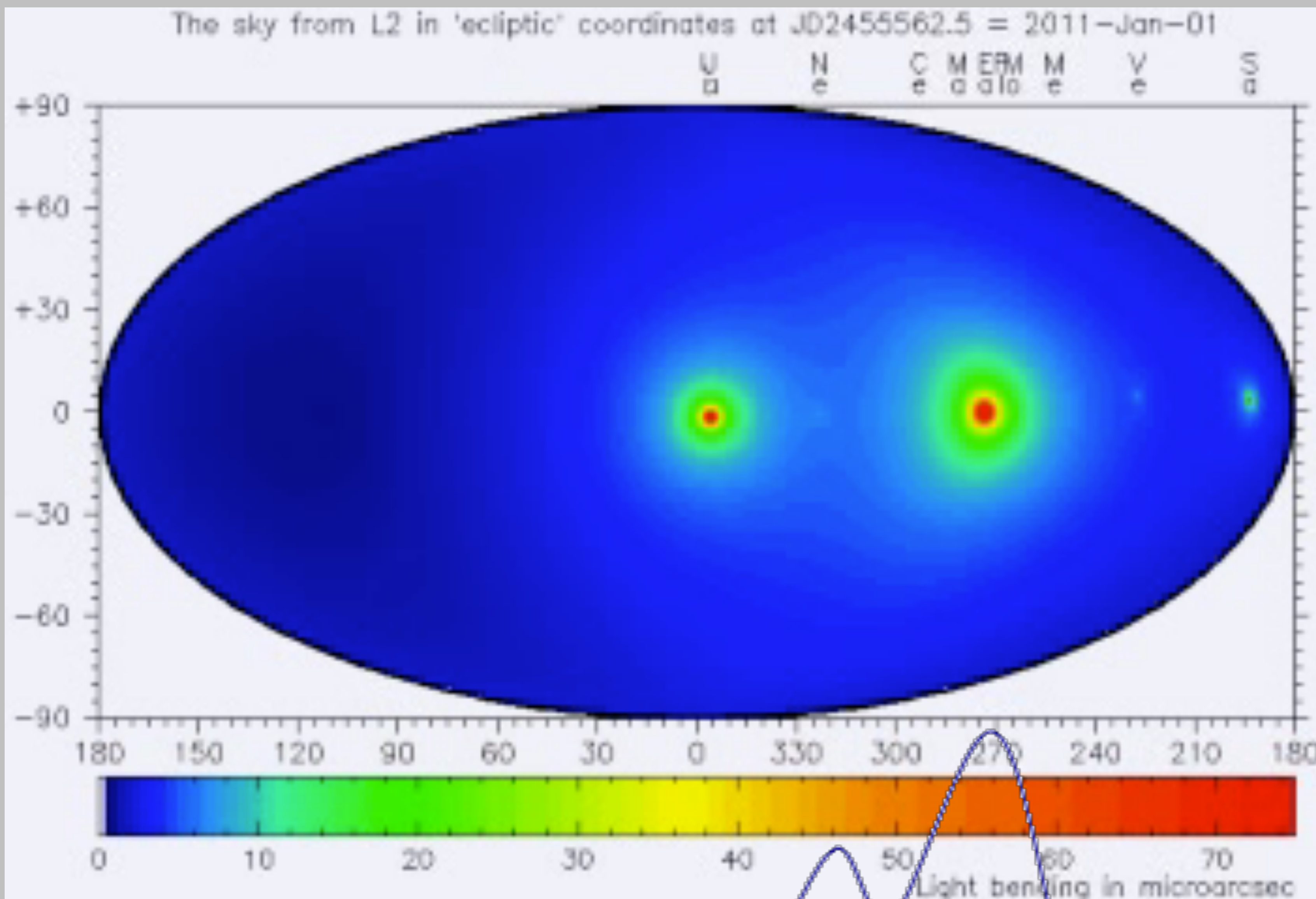

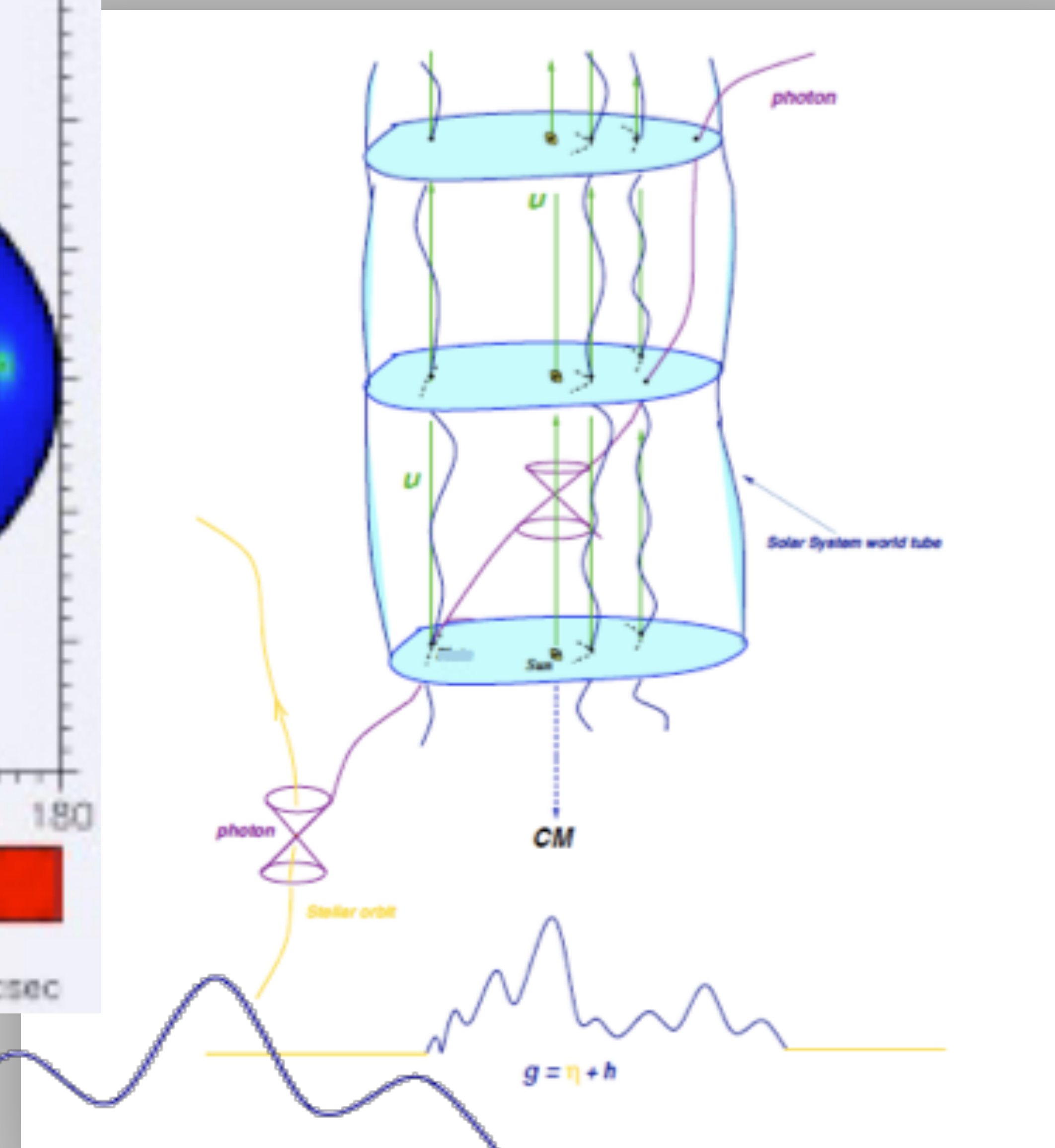

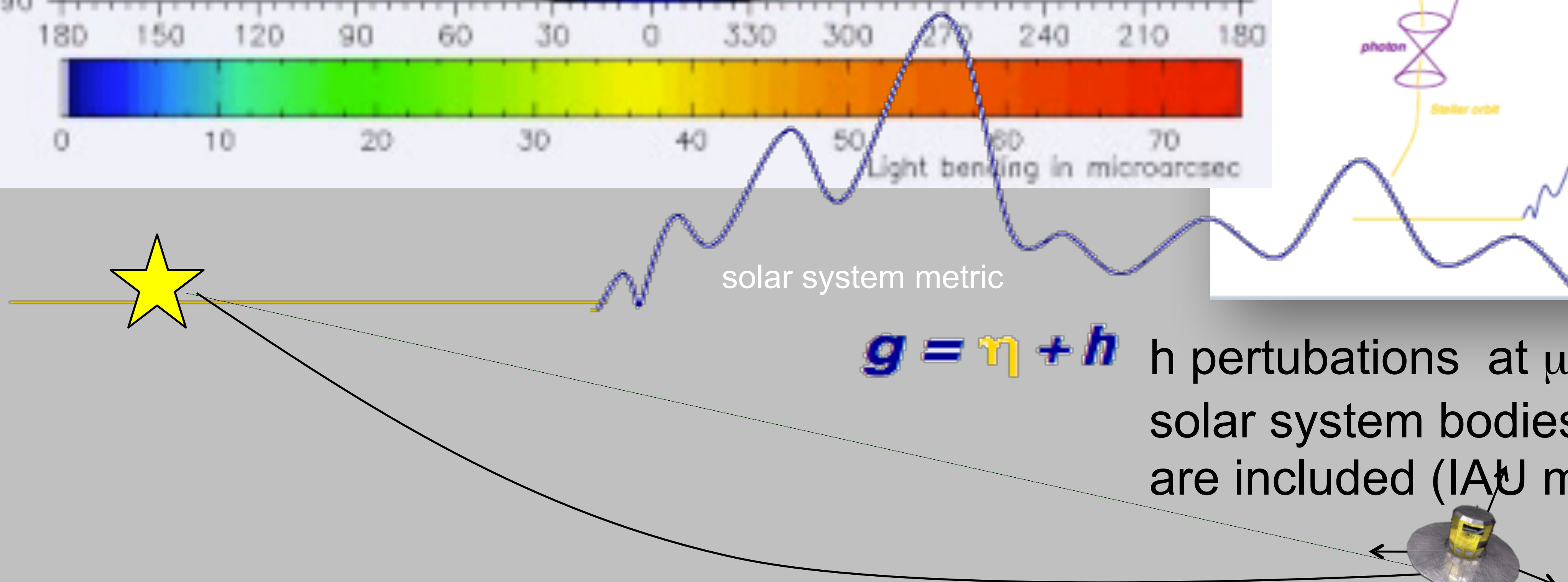

$g = \eta + h$ h pertubations at μ-**arcsec** due to the solar system bodies. Off-diagonal terms are included (IAU metric)

Detectable relativistic deflections at L2 at 1-PN level for grazing light ray

Body	$\delta\alpha_M$ (μas)	$\delta\alpha_Q$ (μas)
Sun	1.75×10^6	~ 1
Mercury	83	
Venus	493	
Earth	574	0.6
Moon	26	
Mars	116	0.2
Jupiter	16270	240
Saturn	5780	95
Uranus	2080	8
Neptune	2533	10

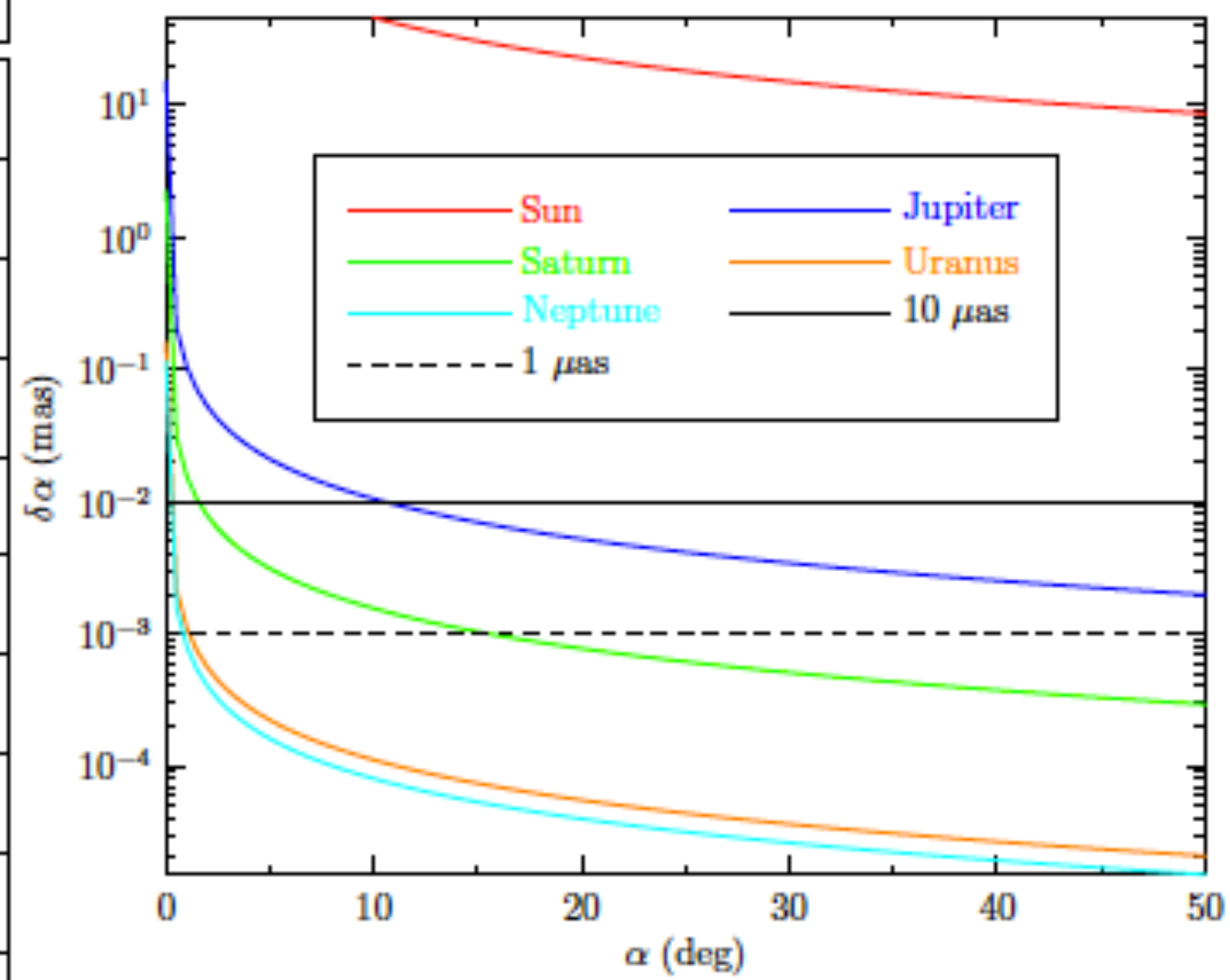

Courtesy of A.Vecchiato

Detectable relativistic deflections at L2 at 1-PN level for grazing light ray

Body	$\delta\alpha_M$ (μas)	$\delta\alpha_Q$ (μas)
Sun	1.75×10^6	~ 1
Mercury	83	
Venus	493	
Earth	574	0.6
Moon	26	
Mars	116	0.2
Jupiter	16270	240
Saturn	5780	95
Uranus	2080	8
Neptune	2533	10

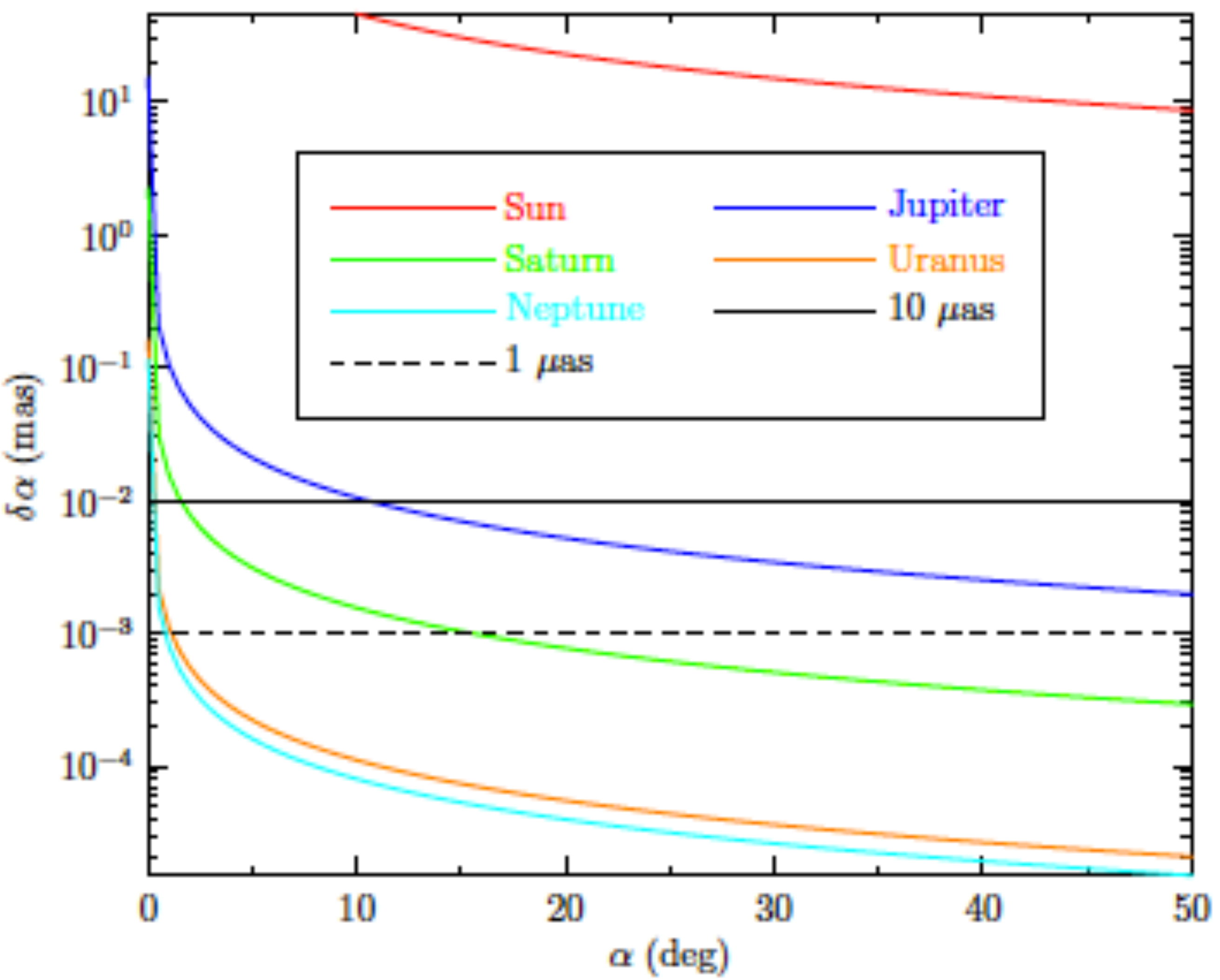

Courtesy of A.Vecchiato

Relativistic astrometry implies a full general-relativistic analysis of the light trajectory, from the observer to the star

~ v^2/c^2 ~ GM/rc^2 ~ mas accuracy

which requires determination of

g_{00} even terms in ε, lowest order ε²~mas

g_{0j} odd terms in ε, lowest order ε³~μ-as

g_{ij} even terms in ε, lowest order ε²~mas

$v/c \sim 10^{-4}\mathrm{rad}$

$$\epsilon = v/c \sim 20.6265''$$

$$\epsilon^2 = (v/c)^2 \sim 2.06265\ \mathrm{mas}$$

$$\epsilon^3 = (v/c)^3 \sim 0.206265\ \mu\mathrm{as}$$

For the Solar System

$$g_{\alpha\beta} = \eta_{\alpha\beta} + h_{\alpha\beta} + O(h^2)$$

$$|h_{\alpha\beta}| \leq U/c^2 \sim v^2/c^2$$

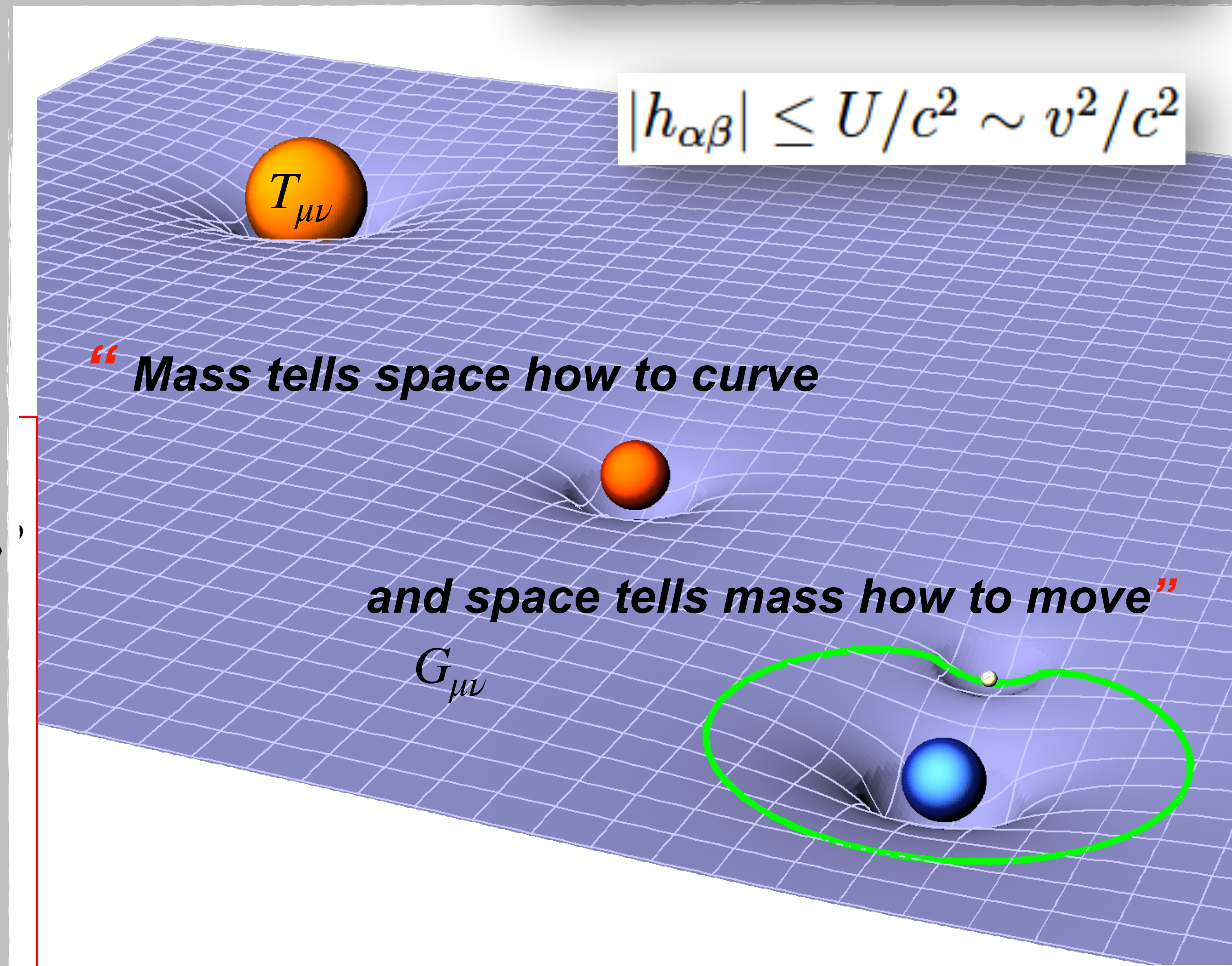

$$g_{00} = -1 + \frac{2}{c^2} w(t,\boldsymbol{x}) - \frac{2}{c^4} w^2(t,\boldsymbol{x}),$$

$$g_{0i} = -\frac{4}{c^3} w^i(t,\boldsymbol{x}),$$

$$g_{ij} = \delta_{ij}\left(1 + \frac{2}{c^2} w(t,\boldsymbol{x})\right).$$

IAU metric for celestial reference system!

Used to describe the motion of celestial bodies and the light propagation

Ephemeris **Relativistic Astrometry**

Gaia, the ESA cornerstone mission, is a wide European effort involving almost 450 scientists, launched in 2013.

2 independent GR models (GREM and RAMOD)-> the Consortium constitued for the Gaia data reduction (DPAC) agreed to set up, respectively, two independent global sphere solutions: AGIS and GSR**.**

The DPCT hosts the systems of the Astrometric Verification Unit (AVU), run by ALTEC (To) under the scientific supervision of the astrometric group INAF-OATo for ASI

All Gaia operations activities (daily and cyclic) done in Italy are implemented at the DPCT, the Italian provided HW and SW operations system designed, built and run by ALTEC (To) and INAF-OATo for ASI.

Size at completion ~ 2 PB

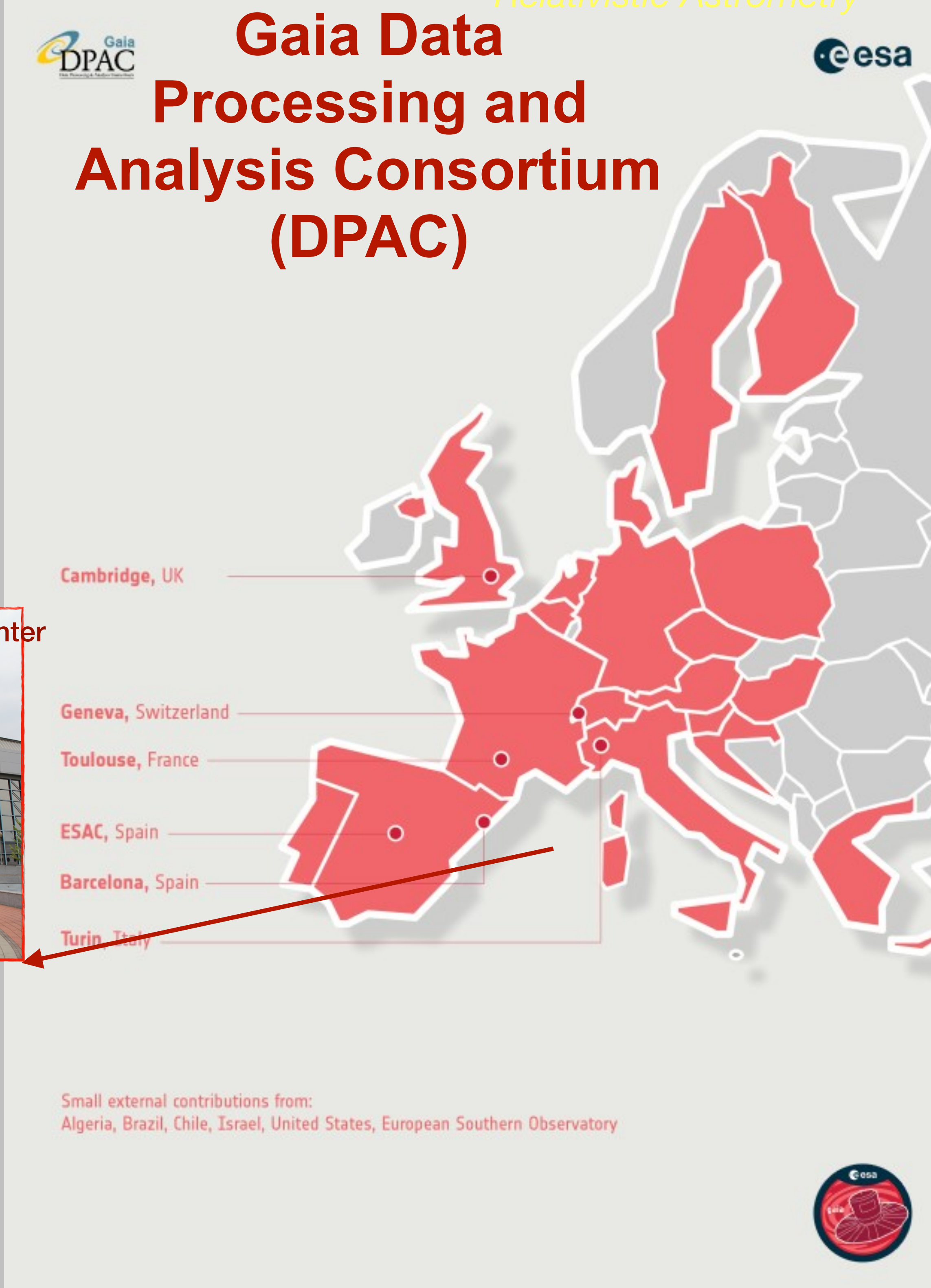

AVU is in charge, for DPAC, of the verification, through the Global Sphere Reconstruction (GSR), of the absolute astrometry achieved through the baseline astrometric model

This is the only Data Processing Center, among the six DPCs across Europe, which specializes in the treatment and validation of the satellite astrometric data -> **a big archive of raw data to exploit**!

The astrometric observable in RAMOD/AVU

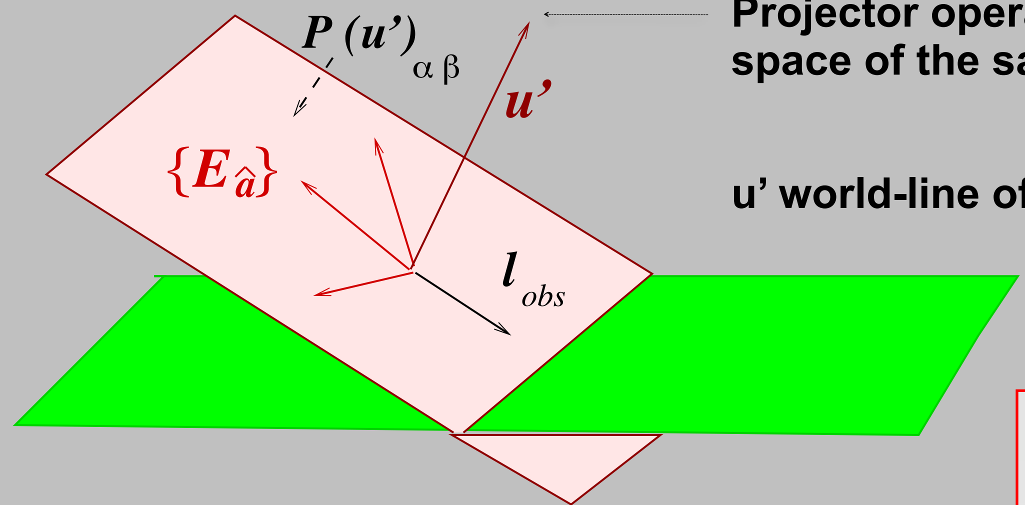

Projector operator onto the rest space of the satellite

u' world-line of the satellite

$E_\alpha{}^\beta$ "attitude tetrad"-> essential to define the boundary condition

Bini , Crosta, and de Felice, Class.Quantum Grav. 20, 4695, 2003

$$\cos\psi_{(E_{\hat{a}},\ell_{obs})} \equiv \mathbf{e}_{\hat{a}} = \frac{P(u')_{\alpha\beta}k^{\alpha}\boldsymbol{E}^{\beta}_{\hat{a}}}{(P(u')_{\alpha\beta}k^{\alpha}k^{\beta})^{1/2}}$$

Observation equation

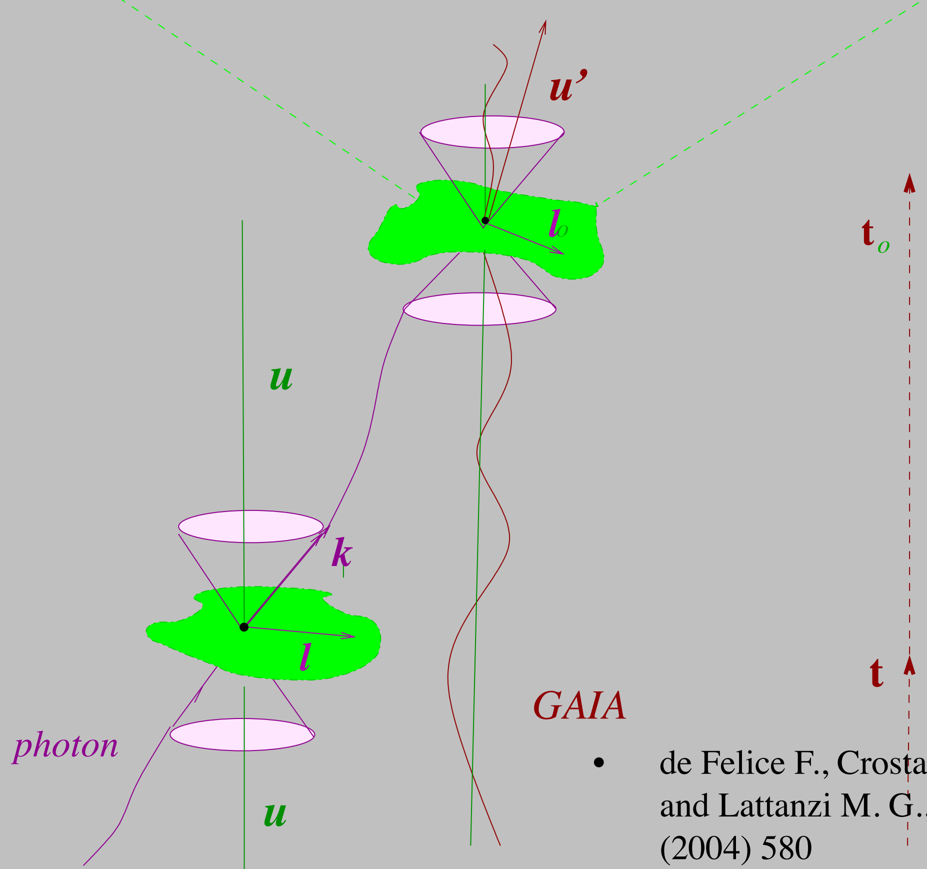

- de Felice F., Crosta M., Vecchiato A. and Lattanzi M. G., Astrophys. J., 607 (2004) 580
- Crosta M., Geralico A., Lattanzi M. G. and Vecchiato A., Phys. Rev. D, 96 (2107) 104030.

The astrometric observable in RAMOD/AVU

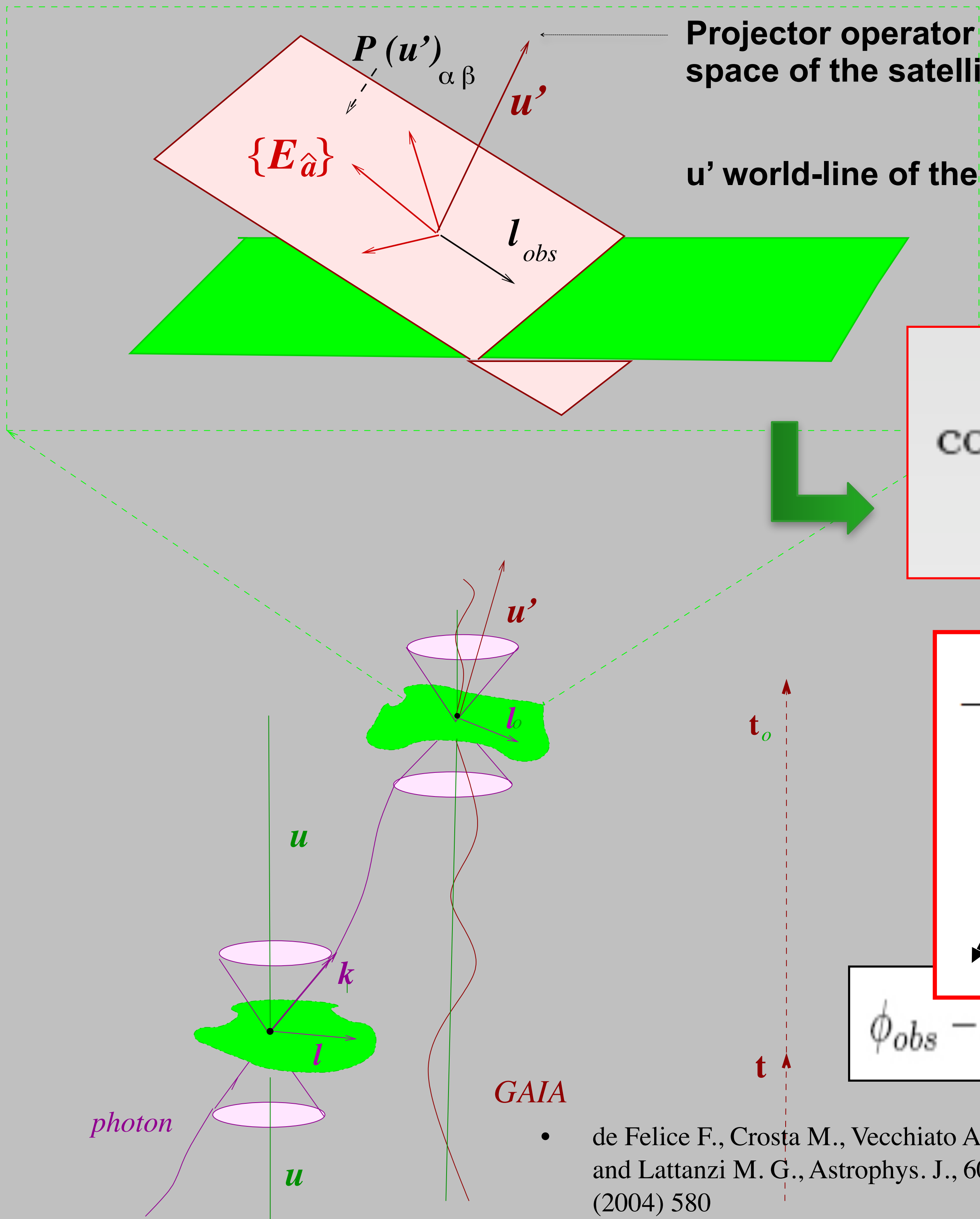

Projector operator onto the rest space of the satellite

u' world-line of the satellite

$E_\alpha^{\ \beta}$ **"attitude tetrad"->** essential to define the boundary condition

Bini , Crosta, and de Felice, Class.Quantum Grav. 20, 4695, 2003

$$\cos\psi_{(E_{\hat{a}},\ell_{obs})} \equiv \mathbf{e}_{\hat{a}} = \frac{P(u')_{\alpha\beta}k^{\alpha}\boldsymbol{E}^{\beta}_{\hat{a}}}{(P(u')_{\alpha\beta}k^{\alpha}k^{\beta})^{1/2}}$$

Observation equation

$$-\sin\phi\, d\phi = \underbrace{\frac{\partial F}{\partial \alpha_*}\delta\alpha_* + \frac{\partial F}{\partial \delta_*}\delta\delta_* + \frac{\partial F}{\partial \varpi_*}\delta\varpi_* + \cdots}_{\text{Astrometric parameters}}$$

$$\sum_{ij}\frac{\partial F}{\partial \sigma_i^{(j)}}\delta\sigma_i^{(j)} + \sum_i \frac{\partial F}{\partial c_i}\delta c_i + \frac{\partial F}{\partial \gamma}\delta\gamma + \cdots$$

$$\phi_{obs} - \phi_{calc}$$

All derivatives are calculated at appropriate "catalog" values

$$\mathbf{x}_* = \frac{1}{\varpi}(\cos\alpha\cos\delta, \sin\alpha\cos\delta, \sin\delta)$$

- de Felice F., Crosta M., Vecchiato A. and Lattanzi M. G., Astrophys. J., 607 (2004) 580
- Crosta M., Geralico A., Lattanzi M. G. and Vecchiato A., Phys. Rev. D, 96 (2107) 104030.
- Vecchiato A. et al., Astron. Astrophys., 620 (2018) A40

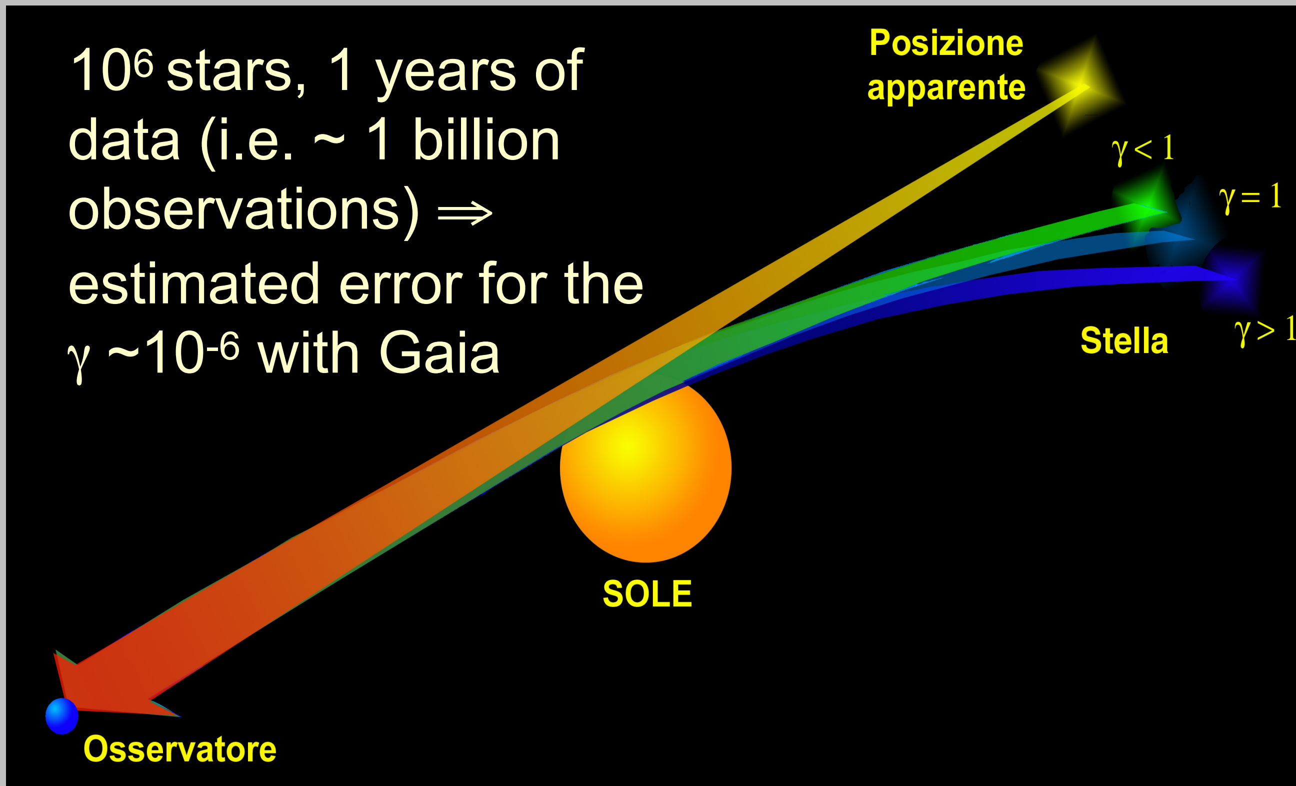

(Vecchiato, et al. 2003, A&A)

with **DR2/EDR3** too many sistematic errors, final calibrations including bright stars will improve the measurements of gamma deviation from one

→ *given the number of celestial objects (a real Galilean method applied on the sky!) and directions involved (the whole celestial sphere!), the largest experiment in General Relativity ever made with astrometric methods (since 1919) from space*

A massive repetition of the Eddington et al. astrometric test of GR with 21st century technology, <u>thank to the interfacing of analytical&numerical relativity methods!</u>

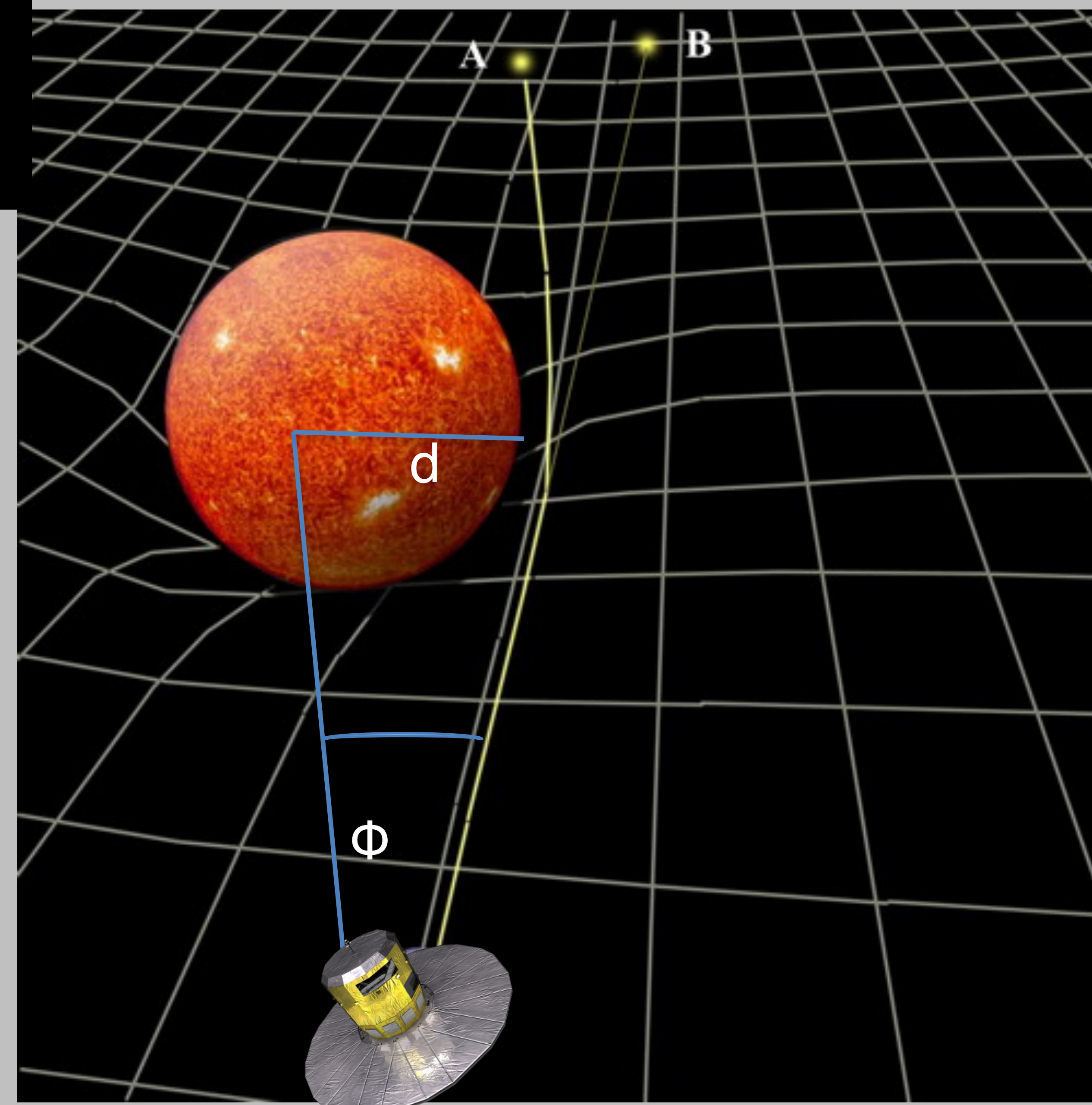

Gravitational astrometry at Milky Way scale

Gaia is delivering a relativistic kinematic

For the Gaia-like observer the weak gravitational regime turns out to be "strong" when one has to perform high accurate measurements

- the position and velocity data, comprising the outputs of the Gaia mission, are fully GR compliant

—>> Given a relativistic approach for the data analysis and processing, any subsequent exploitations should be consistent with the precepts of the theory underlying the astrometric model.

A **fully relativistic model for the Milky Way (MW)** structure should be pursued!

The GR picture of the MW can ensure a coherent Local Cosmology laboratory against which any model of the Galaxy can be fully tested

➢ **Local Cosmology:** how well distances and kinematics at the scale of the Milky Way disk compare with the Lambda-CDM model predictions

In most cosmological simulations ray-tracing is missing, Gaia can provides values (true observables) to estimate model parameters

weak field regime @Milky Way scale

weak field regime @Milky Way scale

In general one assumes that:

gravitational potential or “relativistic effects” at the MW scale are usually “small”, then

✓negligible..

weak field regime @Milky Way scale

In general one assumes that:

gravitational potential or “relativistic effects” at the MW scale are usually “small”, then

✓negligible..

✓locally Newton approximation is retained valid at each point..

but

weak field regime @Milky Way scale

In general one assumes that:

gravitational potential or "relativistic effects" at the MW scale are usually "small", then

✓negligible..

✓locally Newton approximation is retained valid at each point..

but $(v_{Gal}/c)^2 \sim 0{,}69 \times 10^{-6}$ (rad) ~ 100 mas

$(v_{Gal}/c)^3 \sim 0{,}57 \times 10^{-9}$ (rad) $\sim 120\mu\mathrm{as}$

the individual astrometric error is $< 100\mu\mathrm{as}$

weak field regime @Milky Way scale

In general one assumes that:
gravitational potential or “relativistic effects” at the MW scale are usually “small”, then

✓negligible..

✓locally Newton approximation is retained valid at each point..

but $(v_{Gal}/c)^2 \sim 0{,}69 \times 10^{-6}$ (rad) ~100 mas

$(v_{Gal}/c)^3 \sim 0{,}57 \times 10^{-9}$ (rad) ~ $120\mu as$

the individual astrometric error is $< 100\mu as$

“weakly” relativistic effect could be relevant

The small curvature limit in General Relativity may not coincide with the Newtonian regime

Compare GR and (Lambda)-CDM model

weak field regime @Milky Way scale

In general one assumes that:
gravitational potential or "relativistic effects" at the MW scale are usually "small", then

✓negligible..

✓locally Newton approximation is retained valid at each point..

but $(v_{Gal}/c)^2 \sim 0{,}69 \times 10^{-6}$ (rad) ~ 100 mas

$(v_{Gal}/c)^3 \sim 0{,}57 \times 10^{-9}$ (rad) $\sim 120\mu as$

the individual astrometric error is $< 100\mu as$

"weakly" relativistic effect could be relevant

The small curvature limit in General Relativity may not coincide with the Newtonian regime

Compare GR and (Lambda)-CDM model

By routinely scanning individual sources throughout the whole sky, Gaia directly measures the (relativistic) kinematics of the stellar component

-> the rotation curve of the MW as a first test for a GR Galaxy with the Gaia data

RC are distinctive feature of spiral galaxies as MW, a sort of kinematical signature

"Classic" Milky Way (MWC) model with Dark matter halo

- Newtonian limit applied for Galactic dynamics -> Poisson's equation

$$\nabla^2\Phi = 4\pi G\rho$$

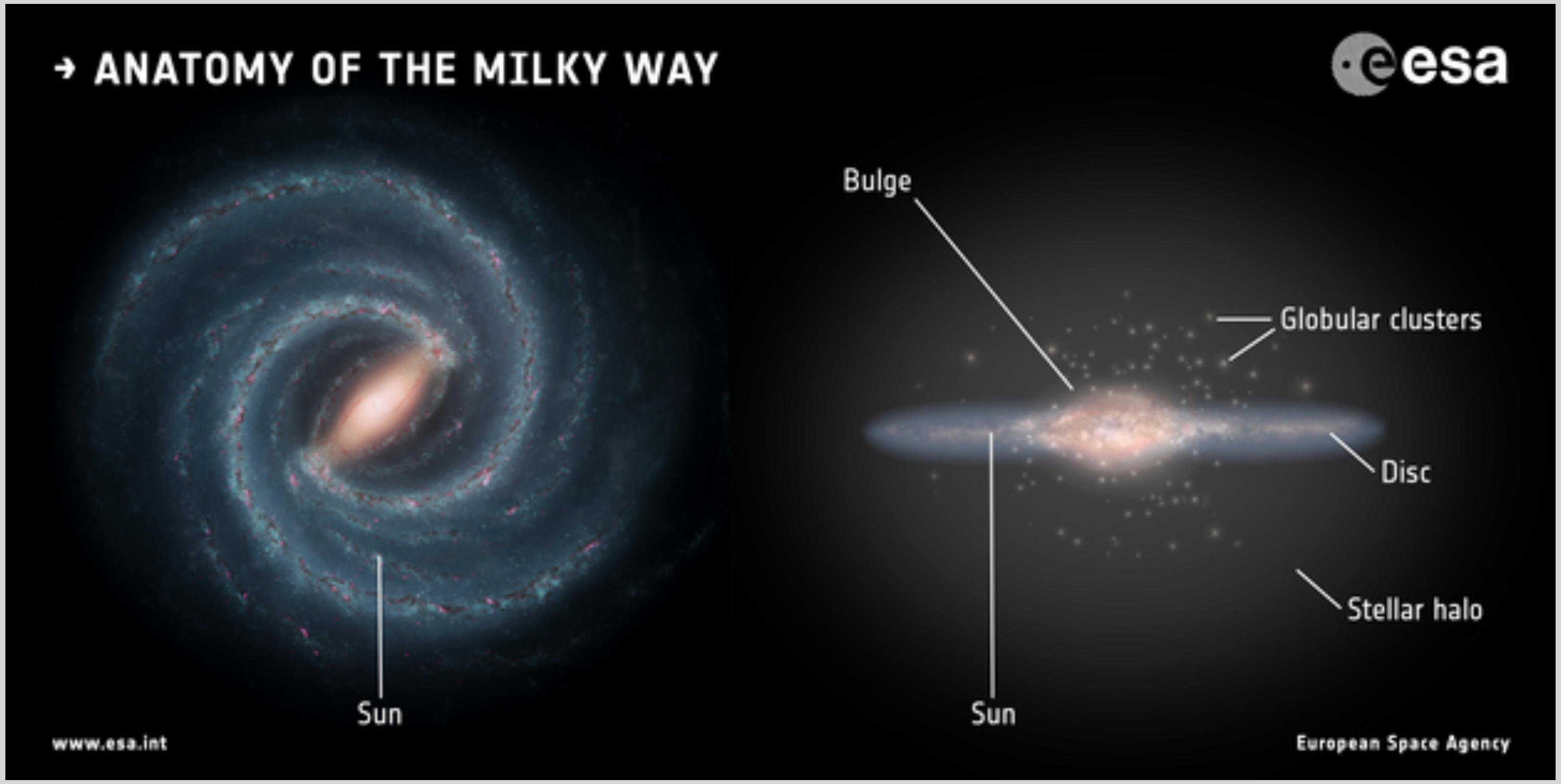

1. Plummer **bulge**

$$\rho_b = \frac{3b_b^2 M_b}{4\pi(r^2 + b_b^2)^{5/2}}$$

bulge spherical radius **b_b=0.3 kpc**

Pouliasis, E., Di Matteo, P., & Haywood, M. 2017, A&A, 598, A66

2. Miyamoto-Nagai **thin and thick disks**

$$\rho_d(R,z) = \frac{M_d b_d^2}{4\pi} \frac{\left[a_d R^2 + (a_d + 3\sqrt{z^2+b_d^2})(a_d+\sqrt{z^2+b_d^2})^2\right]}{\left[R^2 + (a_d + \sqrt{z^2+b_d^2})^2\right]^{5/2} (z^2+b_d^2)^{3/2}}$$

$b_{td} = 0.25$ kpc and $b_{Td} = 0.8$ kpc

Bovy, J. 2015, ApJs, 216, 29 Korol, Rossi & Barausse (2019) McMillan, P. J. 2017, MNRAS, 465, 76-94

3. Navarro-Frank-White DM **halo**

$$\rho_h(r) = \rho_0^{halo} \frac{1}{(r/A_h)(1 + r/A_h)^2}$$

Navarro, J. F., Frenk, C. S. and White, S. D. M. 1996, ApJ, 462, 563

M_b, M_{td}, M_{Td}, a_{td}, a_{Td} , bd, ρ_0^{halo} and **A_h** correspond to the bulge mass, the masses and the scale lengths/heights of the thin and thick disks, the halo scale density, and the halo radial scale

$$\underbrace{\nabla^2\Phi_{tot} = 4\pi G(\rho_b + \rho_{td} + \rho_{Td} + \rho_h)}_{} \Rightarrow V_c^2 = R\left(d\Phi_{tot}/dR\right)$$

MWC velocity profile

GR model for the Milky Way

Einstein equation are very difficult to solve analytically and Galaxy is a multi-structured object making it even the more difficult to detail a metric for the whole Galaxy

$$ds^2 = g_{\alpha\beta}dx^\alpha dx^\beta = -dt^2 + 2Nd\phi dt + (r^2 - N^2)d\phi^2 + e^\nu(dr^2 + dz^2)$$

Galactic metric-disk

1. Stationarity and axisymmetry spacetime
2. Reflection symmetry (around the galactic plane)
3. The disk is an equilibrium configuration of a pressure-less rotating perfect fluid (a GR dust)
4. The masses inside a large portion of the Galaxy interact only gravitationally and reside far from the central bulge region
5. The rotational curve is due to the angular-momentum sustained stellar population
6. Stars = dust grains, co-moving with the Gaia-observer

Einstein field Eq. from the metric disk

$$r\partial_z\nu + \partial_r N \partial_z N = 0$$

$$2r\partial_r\nu + (\partial_r N)^2 - (\partial_z N)^2 = 0$$

$$2r^2(\partial_r\partial_r\nu + \partial_z\partial_z\nu) + (\partial_r N)^2 + (\partial_z N)^2 = 0$$

$$r(\partial_r\partial_r N + \partial_z\partial_z N) - \partial_r N = 0$$

$$\boxed{(\partial_r N)^2 + (\partial_z N)^2 = kr^2\rho e^\nu}$$

GR model for the Milky Way

Einstein equation are very difficult to solve analytically and Galaxy is a multi-structured object making it even the more difficult to detail a metric for the whole Galaxy

$$ds^2 = g_{\alpha\beta}dx^\alpha dx^\beta = -dt^2 + 2Nd\phi dt + (r^2 - N^2)d\phi^2 + e^\nu(dr^2 + dz^2)$$

Galactic metric-disk

1. Stationarity and axisymmetry spacetime
2. Reflection symmetry (around the galactic plane)
3. The disk is an equilibrium configuration of a pressure-less rotating perfect fluid (a GR dust)
4. The masses inside a large portion of the Galaxy interact only gravitationally and reside far from the central bulge region
5. The rotational curve is due to the angular-momentum sustained stellar population
6. Stars = dust grains, co-moving with the Gaia-observer

The function $N(r,z)$ was constrained by Balasin & Grumiller (BG) to the separation anstaz $N(r,z) = R(r)F(z)$ and the reflection symmetry assumption.

$$N(r,z) = V_0(R_{out} - r_{in}) + \frac{V_0}{2}\sum_{\pm}\left(\sqrt{(z \pm r_{in})^2 + r^2} - \sqrt{(z \pm R_{out})^2 + r^2}\right)$$

(Balasin and Grummiler, Int.J. Mod. Phys., 2008)

$|z| < r_{in}$

- **r_{in} = bulge size**
- **R_{out} = extension of the MW disk-> Galaxy size**
- **V_0 = velocity in the flat regime**

Einstein field Eq. from the metric disk

$$r\partial_z\nu + \partial_r N \partial_z N = 0$$

$$2r\partial_r\nu + (\partial_r N)^2 - (\partial_z N)^2 = 0$$

$$2r^2(\partial_r\partial_r\nu + \partial_z\partial_z\nu) + (\partial_r N)^2 + (\partial_z N)^2 = 0$$

$$r(\partial_r\partial_r N + \partial_z\partial_z N) - \partial_r N = 0$$

$$\boxed{(\partial_r N)^2 + (\partial_z N)^2 = kr^2\rho e^\nu}$$

$$\rho(R,z) = e^{-\nu(R,z)}\frac{1}{8\pi R^2}\left[\left(\partial_R N(R,z)\right)^2 + \left(\partial_z N(R,z)\right)^2\right]$$

The Gaia observer linked to the gravitational dragging

Observer in circular motion

$$u^\alpha = \Gamma\left(k^\alpha + \beta m^\alpha\right)$$

β constant angular velocity (with respect to infinity), Γ normalization factor

or

$$u^\alpha = \gamma\left(e^\alpha_{\hat{0}} + \zeta^{\hat{\phi}} e^\alpha_{\hat{\phi}}\right)$$

ZAMO frames = locally non-rotating observers, zero angular momentum with respect to flat infinity and move on worldlines orthogonal to the hypersurfaces t=constant

γ Lorentz factor

orthonormal frame adapted to the ZAMO $Z^\alpha = (1/M)(\partial_t - M^\phi \partial_\phi)$ $M = r/\sqrt{(r^2 - N^2)}$, $M^\phi = N/(r^2 - N^2)$

(de Felice and Bini, "Classical measurements in curved space-time")

$$\zeta^{\hat{\phi}} = \frac{\sqrt{g_{\phi\phi}}}{M}(\beta + M^\phi)$$

$$ds^2 = -M^2 dt^2 + (r^2 - N^2)\left(d\phi + M^\phi dt\right)^2 + e^\nu(dr^2 + dz^2)$$

$$\zeta^{\hat{\phi}} = \frac{N(r,z)}{r}$$

if static (<u>as the observer in BCRS, Gaia catalogue</u>)

Crosta M., Giammaria M., Lattanzi M. G., Poggio E., (2020)

$$\boxed{V(r,z) = N(r,z)/r \propto g_{0\phi}}$$

V: spatial velocity of the co-rotating dust as seen by an asymptotic observer at rest wrt to the center of the Galaxy (or the rotation axis)

Gravitational dragging working at disk scale

The question before us: the MW rotation curve, dark matter or geometry driven?

Data sample: full reconstruction of disc kinematics based on DR2 data only

i. **Complete Gaia DR2 astrometric dataset** ($\alpha, \delta, \mu_\alpha, \mu_\delta$,parallax)
ii. **Parallaxes good to 20%** (i.e. parallax_over_error ≥ 5)
—> parallaxes to better than 20% allow to deal with similar (quasi–gaussian) statistics when transforming to distances
iii. **Gaia-measured velocity along the line of sight,** i.e. **radial velocity, with better than 20% uncertainties** from Gaia DR2

i.+ii.+iii.—> **proper 6D reconstruction of the phase-space location occupied by each individual star as derived by the same observer**

iv. Only for Early Type stars, **cross-matched entry in the 2MASS catalog** following Poggio et al. (2018)
—> for the actual materialization of the sample

1. Full transformation (including complete error propagation) from the ICRS equatorial to heliocentric galactic coordinates
2. then translation to the galactic center

Crosta, Giammaria, Lattanzi, Poggio, MNRAS, 496,(2020)

very homogenous sample of 5277 early type stars and 325 classical type I Cepheids.

99.4 % of the sample in 4,9 ≤ r ≤ 15,8 kpc (a range of 11 kpc) and below 1 kpc from the galactic plane (characteristic scale height for the validity of the BG model)

to date the best angular-momentum sustained stellar population of the Milky Way that better traces its observed RC!

MCMC fit to the Gaia DR2 data - Classical (MWC) and GR (BG) RC

Best fit estimates as the median of the posteriors and their 1σ level credible interval

$$V_\phi^{BG}(R) = \frac{V_0}{R}\left(R_{out} - r_{in} + \sqrt{r_{in}^2 + R^2} - \sqrt{R_{out}^2 + R^2}\right)$$

BG model	θ	σ_θ^-	σ_θ^+
r_{in} [kpc]	0.39	-0.25	+0.36
R_{out} [kpc]	47.87	-14.80	+23.96
V_0 [km/s]	263.10	-16.44	+25.93
e^{ν_0}	0.083	- 0.014	+0.014

MWC model	θ	σ_θ^-	σ_θ^+
$M_b[10^{10}M_\odot]$	1.0	-0.4	+0.4
$M_{td}[10^{10}M_\odot]$	3.9	-0.4	+0.4
$M_{Td}[10^{10}M_\odot]$	4.0	-0.5	+0.5
a_{td}[kpc]	5.2	-0.5	+0.5
a_{Td}[kpc]	2.7	-0.4	+0.4
$\rho_0^{halo}[M_\odot pc^{-3}]$	0.009	-0.003	+0.004
A_h [kpc]	17	-3	+4

Both models fit the data!

Colored area= reliability intervals of the fitted curves

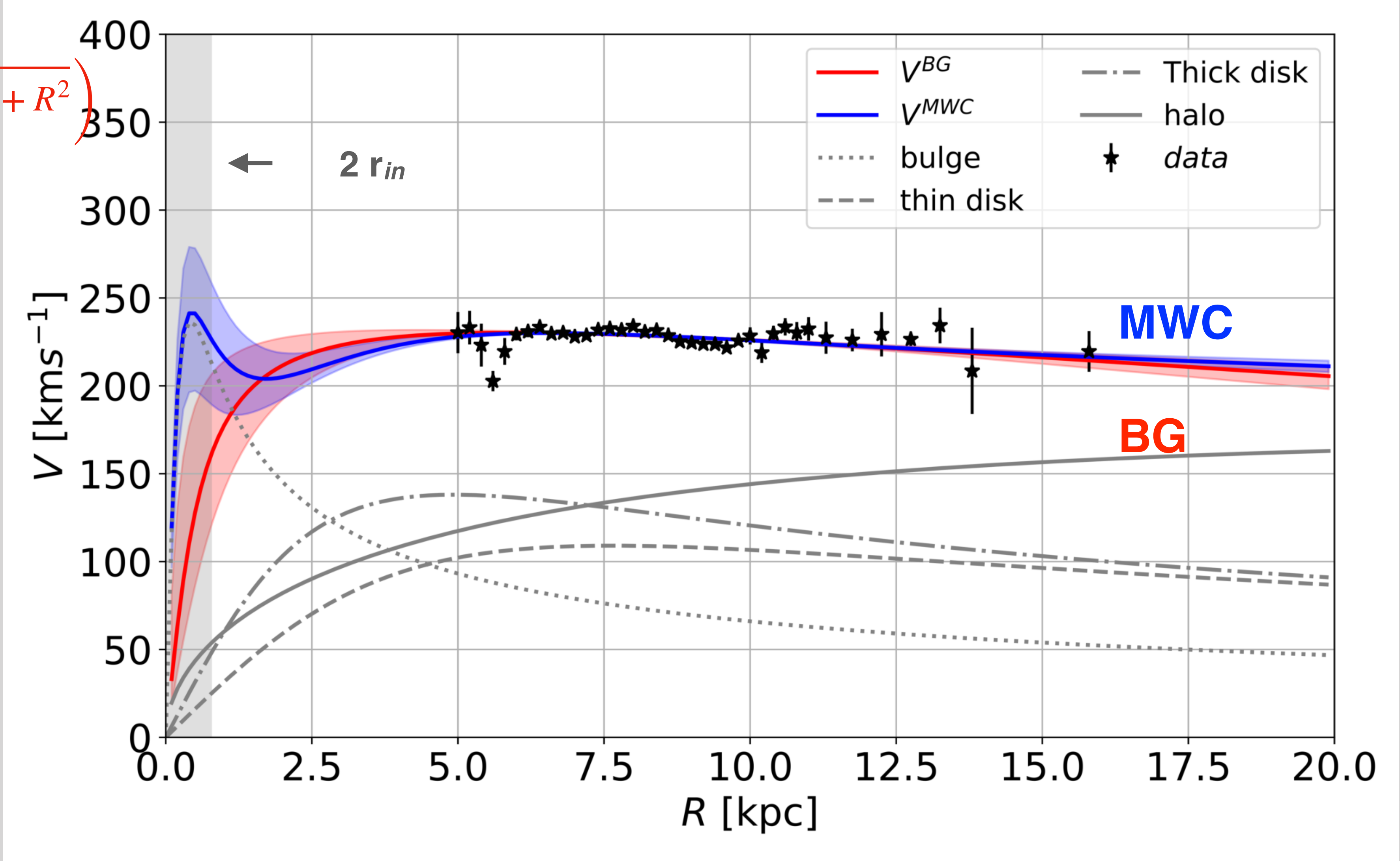

For our likelihood analysis the two models appear almost identically consistent with the data.

Weak field GR off-diagonal term mimic DM in MW!

Ref:On testing CDM and geometry-driven Milky Way rotation curve models with *Gaia* DR2- Crosta M., Giammaria M., Lattanzi M. G., Poggio E.,MNRAS, Volume 496, Issue 2, August 2020, Pages 2107–2122

For both models, the errors due to the Bayesian analyses are at least one order of magnitude lower than the resulting uncertainties of the parameters.

For the BG free parameters uniform prior distributions (first general relativistic model fitted to data)

For MWC normal prior distributions (comparison of our bayesian analysis with the most recent observational estimates)

MCMC fit to the Gaia DR2 data - Classical (MWC) and GR (BG) RC

Both models fit the data! Colored area= reliability intervals of the fitted curves

Best fit estimates as the median of the posteriors and their 1σ level credible interval

$$V_\phi^{BG}(R) = \frac{V_0}{R}\left(R_{out} - r_{in} + \sqrt{r_{in}^2 + R^2} - \sqrt{R_{out}^2 + R^2}\right)$$

BG model	θ	σ_θ^-	σ_θ^+
r_{in} [kpc]	0.39	b_b=0.3 kpc!	+0.36
R_{out} [kpc]	47.87	-14.80	+23.96
V_0 [km/s]	263.10	-16.44	+25.93
e^{ν_0}	0.083	- 0.014	+0.014

MWC model	θ	σ_θ^-	σ_θ^+
$M_b[10^{10}\mathrm{M}_\odot]$	1.0	-0.4	+0.4
$M_{td}[10^{10}\mathrm{M}_\odot]$	3.9	-0.4	+0.4
$M_{Td}[10^{10}\mathrm{M}_\odot]$	4.0	-0.5	+0.5
a_{td}[kpc]	5.2	-0.5	+0.5
a_{Td}[kpc]	2.7	-0.4	+0.4
$\rho_0^{halo}[\mathrm{M}_\odot\mathrm{pc}^{-3}]$	0.009	-0.003	+0.004
A_h [kpc]	17	-3	+4

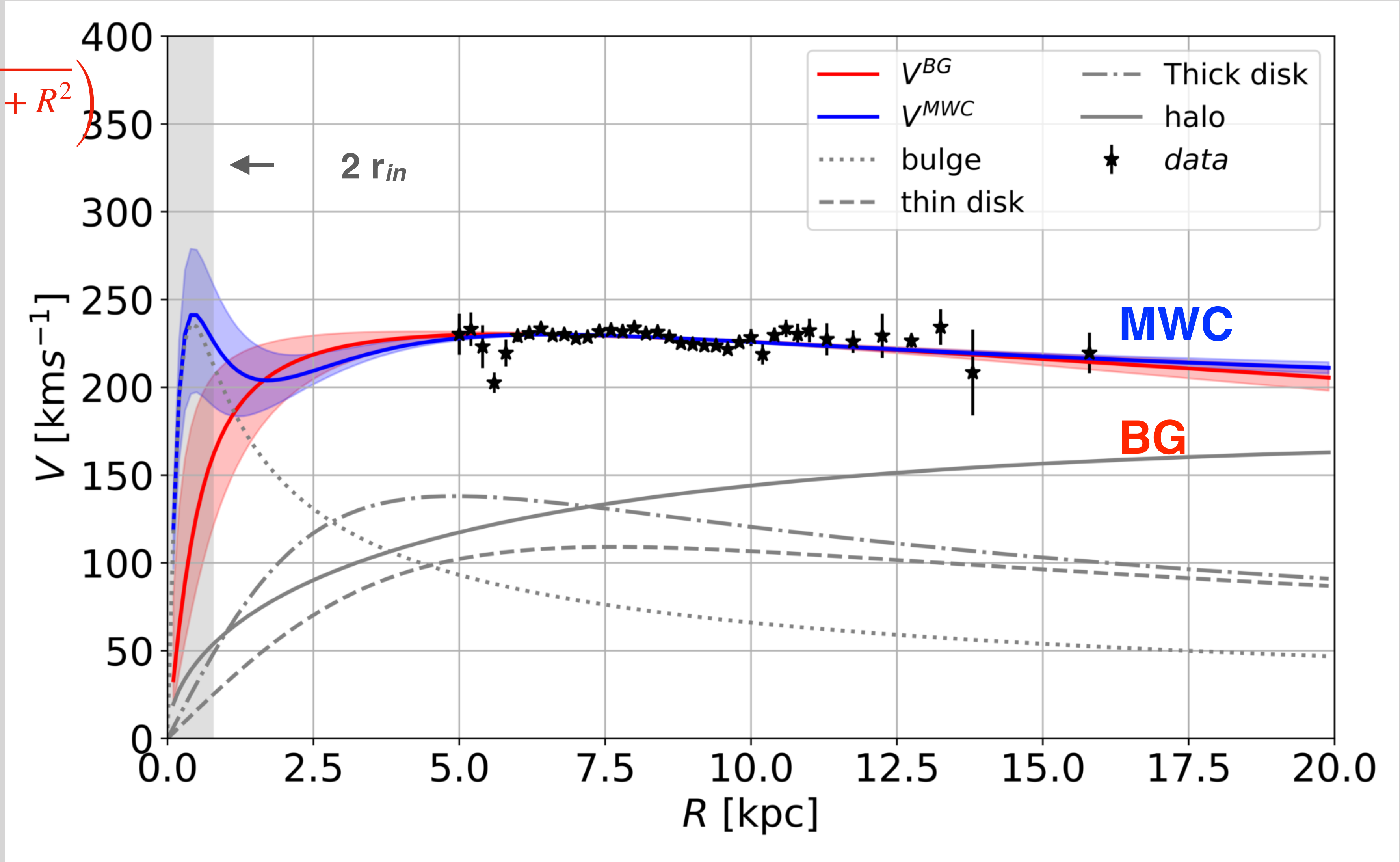

For our likelihood analysis the two models appear almost identically consistent with the data.

Weak field GR off-diagonal term mimic DM in MW!

Ref:On testing CDM and geometry-driven Milky Way rotation curve models with *Gaia* DR2- Crosta M., Giammaria M., Lattanzi M. G., Poggio E.,MNRAS, Volume 496, Issue 2, August 2020, Pages 2107–2122

For both models, the errors due to the Bayesian analyses are at least one order of magnitude lower than the resulting uncertainties of the parameters.

For the BG free parameters uniform prior distributions (first general relativistic model fitted to data)

For MWC normal prior distributions (comparison of our bayesian analysis with the most recent observational estimates)

The baryonic density profile via Einstein field eq.

According to the relativistic model

$$0.083 \pm 0.006$$

solar masses/cubic parsec

In agreement, with current independent estimates

0.077±0.007 Msun pc^{-3}
(Bienayme et al. 2014, A&A, 571)

0.084 ± 0.012 Msun pc^{-3}
(McKee et al. 2015, ApJ, 814, 13)

$0.098^{+0.006}$ Msun pc^{-3}
(Garbari et al. 2012MNRAS, 425, 1445)

As expected in the disk region ($z \sim 0$), for MWC the dominant matter is baryonic, while DM is a minor component there, i.e. $\rho_{DM} \sim 0.01 M_{\odot} pc^{-3}$

$$\rho(R,z) = e^{-\nu(R,z)} \frac{1}{8\pi R^2} \left[\left(\partial_R N(R,z)\right)^2 + \left(\partial_z N(R,z)\right)^2 \right]$$

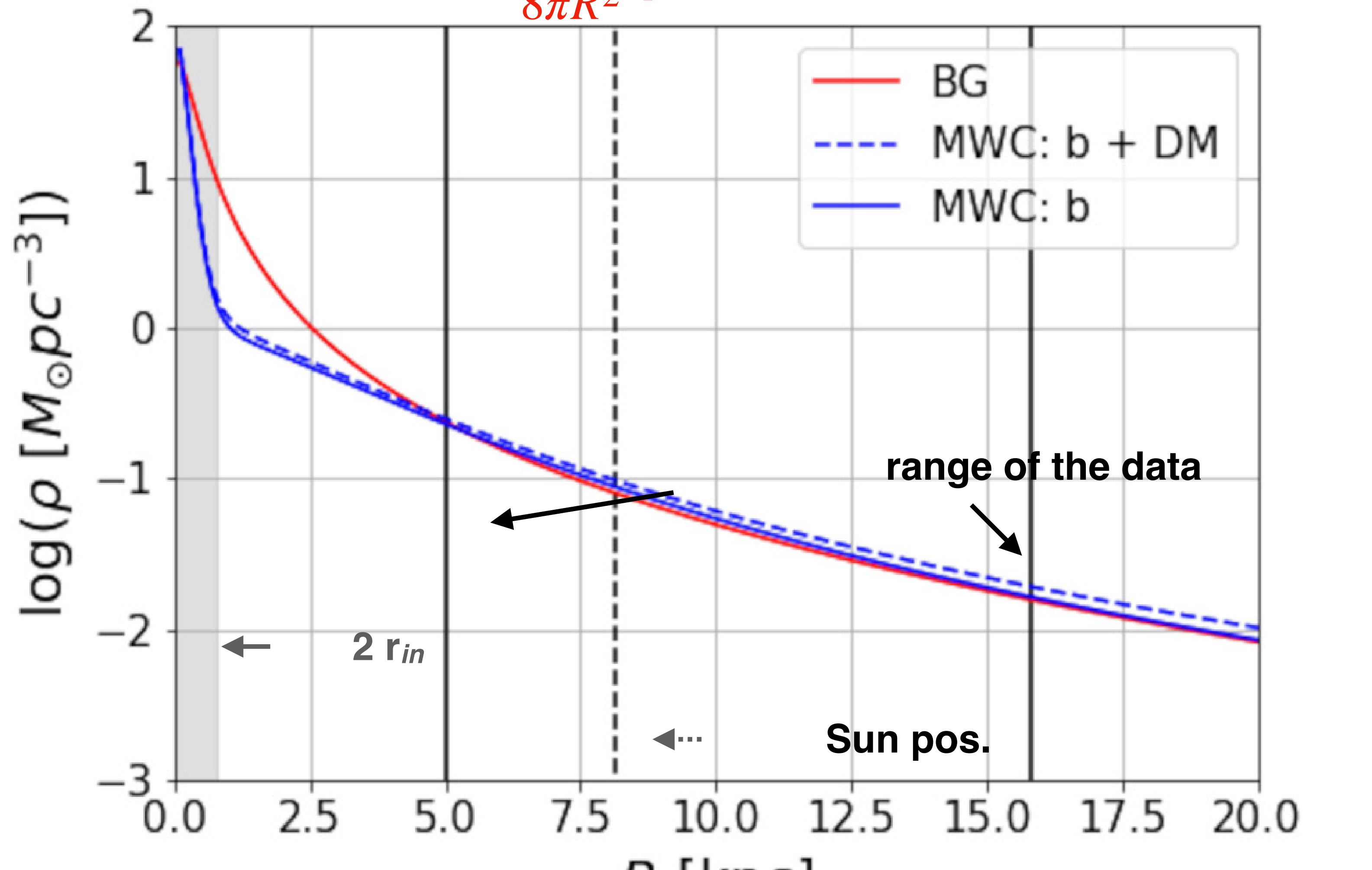

Crosta et al.MNRAS (2020)

Density profile of the MW at z=0 derived from 100 random draws from the posterior distribution of the fit

$$\begin{aligned} \log \mathcal{L} &= -\frac{1}{2} \sum_i \left(\frac{[V_\phi(R_i) - V_\phi^{exp}(R_i|\theta)]^2}{\sigma^2_{V_\phi}} + \log\left(\sigma^2_{V_\phi}\right) \right) \\ &- \frac{1}{2} \left(\frac{[\rho(R_\odot) - \rho^{exp}(R_\odot|\theta)]^2}{\sigma^2_{\rho_\odot}} + \log\left(\sigma^2_{\rho_\odot}\right) \right) \end{aligned}$$

Dragging effect vs. halo effect

The relativistic dragging effect has no newtonian counterpart, thus we compared:

(i) the MWC baryonic-only contribution with the effective Newtonian profile (Binney & Tremaine 1988) calculated by using the BG density: V_{eN}^{BG}

(ii) the MWC dark matter-only contribution (halo) with the "dragging curve" traced by subtracting V_{eN}^{BG} to V_{BG}

$$\sum_i (V_{eN}^{BG}(R_i, k) - V_{eN}^{MWC}(R_i))^2/N \qquad |z_k| < r_{in}$$

For the effective BG disk half- thickness $|z|_{\rm eff}$, the minimization process yields **$|z|_{\rm eff}$=0.215kpc** $b_{\rm td} = 0.25$ **kpc!**

$$\boxed{(V_{drag}^{BG}(R_i; |z|_{eff}|) = \sqrt{(V^{BG}(R))^2 - (V_{eN}^{BG}(R; |z|_{eff}))^2}}$$

amount of rotational velocity across the MW plane <u>due to gravitational dragging</u>

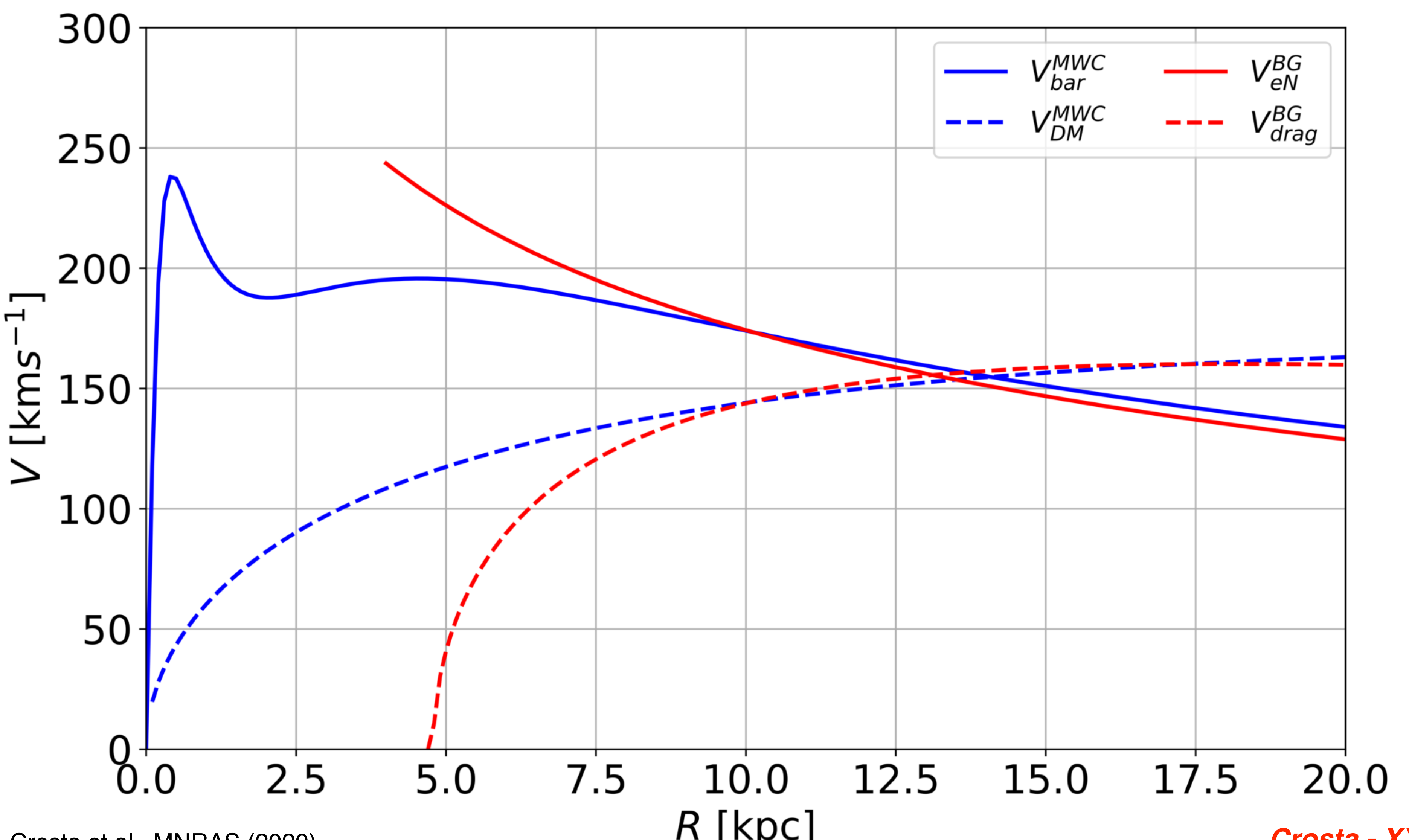

Crosta et al., MNRAS (2020)

R < 5 kpc could be the breaking point for the direct applicability of the BG model to the Milky Way, as it calls for a more suitable relativistic description of its central regions

Dragging effect vs. halo effect

The relativistic dragging effect has no newtonian counterpart, thus we compared:

(i) the MWC baryonic-only contribution with the effective Newtonian profile (Binney & Tremaine 1988) calculated by using the BG density: V_{eN}^{BG}

(ii) the MWC dark matter-only contribution (halo) with the "dragging curve" traced by subtracting V_{eN}^{BG} to V_{BG}

$$\sum_i (V_{eN}^{BG}(R_i, k) - V_{eN}^{MWC}(R_i))^2/N \qquad |z_k| < r_{in}$$

For the effective BG disk half- thickness $|z|_{eff}$, the minimization process yields **$|z|_{eff}$=0.215kpc** $\quad$ **b_{td} = 0.25 kpc!**

$$\boxed{(V_{drag}^{BG}(R_i; |z|_{eff}|) = \sqrt{(V^{BG}(R))^2 - (V_{eN}^{BG}(R; |z|_{eff}))^2}}$$

amount of rotational velocity across the MW plane <u>due to gravitational dragging</u>

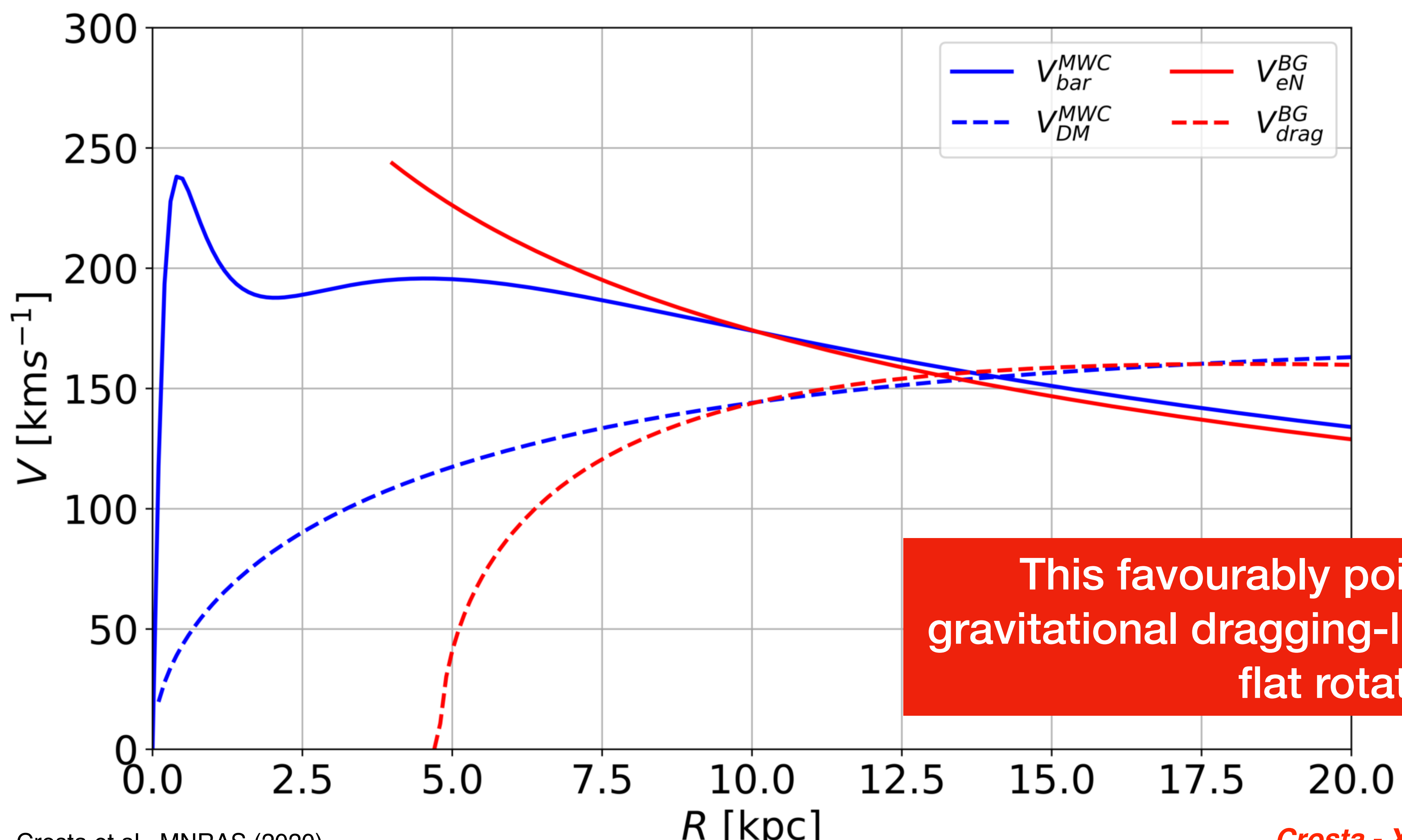

Crosta et al., MNRAS (2020)

R < 5 kpc could be the breaking point for the direct applicability of the BG model to the Milky Way, as it calls for a more suitable relativistic description of its central regions

This favourably points to the fact that a gravitational dragging-like effect could sustain a flat rotation curve

Hypotheses non fingo & Occam's razor

Our interpretation of the fitted relativistic velocity profile with Gaia DR2
depends only on the background geometry

DM: does not absorb or emit light but it exerts and responds only to the gravity force; it enters the calculation as extra mass (halo) required to justify the flat galactic rotational curves.

GR: a gravitational dragging "DM-like" effect driving the Galaxy velocity rotation curve could imply that geometry - unseen but perceived as manifestation of gravity according to Einstein's equation - is responsible of the flatness at large Galactic radii.

By setting a coherent GR framework, one can effectively establish

" Mass tells space how to curve and space tells mass how to move"

i.e. to what extent the MW structure is dictated by the standard theory of gravity

Hypotheses non fingo & Occam's razor

Our interpretation of the fitted relativistic velocity profile with Gaia DR2
depends only on the background geometry

DM: does not absorb or emit light but it exerts and responds only to the gravity force; it enters the calculation as extra mass (halo) required to justify the flat galactic rotational curves.

GR: a gravitational dragging "DM-like" effect driving the Galaxy velocity rotation curve could imply that geometry - unseen but perceived as manifestation of gravity according to Einstein's equation - is responsible of the flatness at large Galactic radii.

By setting a coherent GR framework, one can effectively establish

" Mass tells space how to curve and space tells mass how to move"

i.e. to what extent the MW structure is dictated by the standard theory of gravity

the "ether" was cured by a new kinematics (i.e. special relativity) instead of "new" dynamic as inspired by the FitzGerald-Lorentz contraction phenomena ("extra molecular force")
"*We know that electric forces are affected by the motion of the electrified bodies relative to the ether and it seems a not improbable supposition that the molecular forces are affected by the motion and that the size of the body alters consequently."* FitzGerald, Science, 1889

Next improvements

In 2022, at the time of the Gaia 3rd release, DR3, extension of test with the rotation curve by another 2-4 kpc (including both sides, inner and outer, of the MW disk).

For the **observational side**

- Increase the sample: Gaia eDR3/DR3 (2022) + spectroscopic surveys (e.g. SDSS, APOGEE, LAMOST, RAVE, GES - Gaia ESO Survey, GALAH)
- Match with observations toward the Galactic center
- Expected sample size to increase from current 6000 to more than 100 thousands upper main sequence disc stars, with the addition of early-type B stars.

For the **theoretical side**

- Improve the model: new solutions & new observables of the Einstein Field Equation (i.e. metric solutions to describe the Galaxy); a more consistent mathematical solution of a relativistic velocity profile; a study, e.g., of the class of Lewis and Papapertou metrics in attempt to encompass all the different MW structures and to fit different conformal factors with the Gaia data (as we did for the density in BG case)
- Extend the MW “geometry” to other galaxies, including also relativistic kinematic
- Comparison with N-body (cosmological) simulations also with numerical relativity (e.g. Einstein-Vlasov system solvers). The use of Gaia data must be parallel with the utilisation of the most advanced cosmological simulations with baryonic matter (gas and stars)

With more physically appropriate metrics, along with mathematical adequate solution, the Galaxy can play a reference role for other galaxies, much like the Sun for stellar models

NEW LOCAL TESTS: GAREQ (GAia Relativistic Experiment on Quadrupole, light deflection by Jupiter's quadrupole)

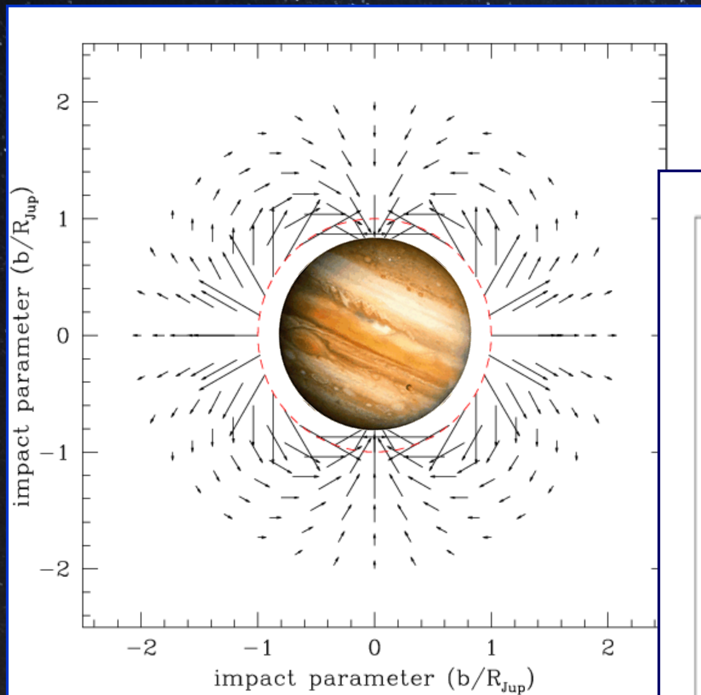

$$\Delta\Phi = \Delta\Phi_1 \mathbf{n} + \Delta\Phi_2 \mathbf{m}$$

Crosta, Mignard (CqG, 2006)
Crosta, et al.(2008, **GAIA-C3-TN-INAF-MTC-003-1)**

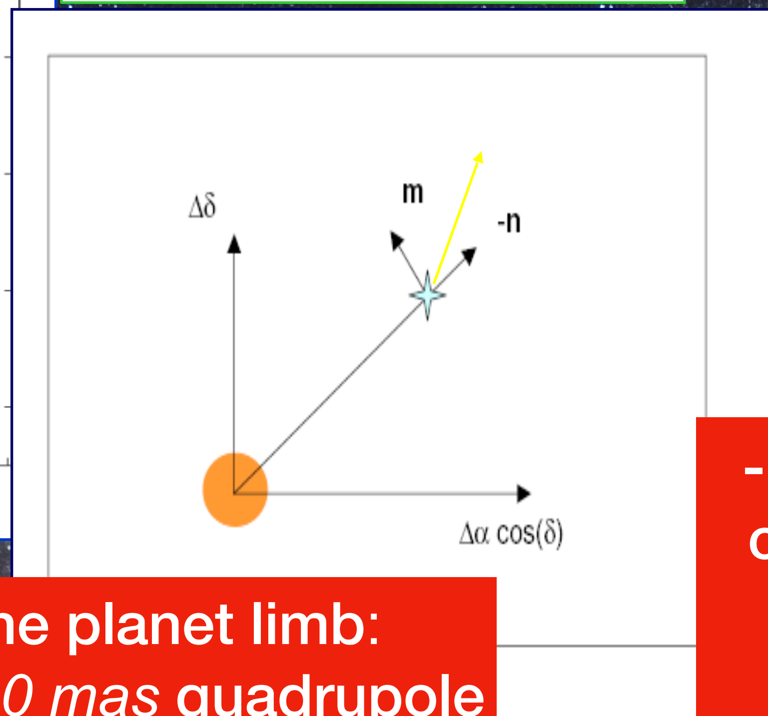

first quantitative measurement of the gravitational potential due to a non-spherical lens

->#Gaia spin axis orientation optimised to catch a star close to the limb of Jupiter in 2017 for a precise light deflection measurement.

GR predictions at the planet limb:
16 mas **monopole,** ***0.240 mas*** **quadrupole**

The follow-up optimization campaign carried out by the dedicated RElativistic Modelling And Testing (REMAT) working group within the Data Processing Analysis Consortium (DPAC) of Gaia with a further fine-tuning of the spin phase led to the predicted favourable configuration of three stars with G < 15.75 mag close to Jupiter's limb for February 2017 (Klioner & Mignard 2014a,b; Abbas et al. 2014). .

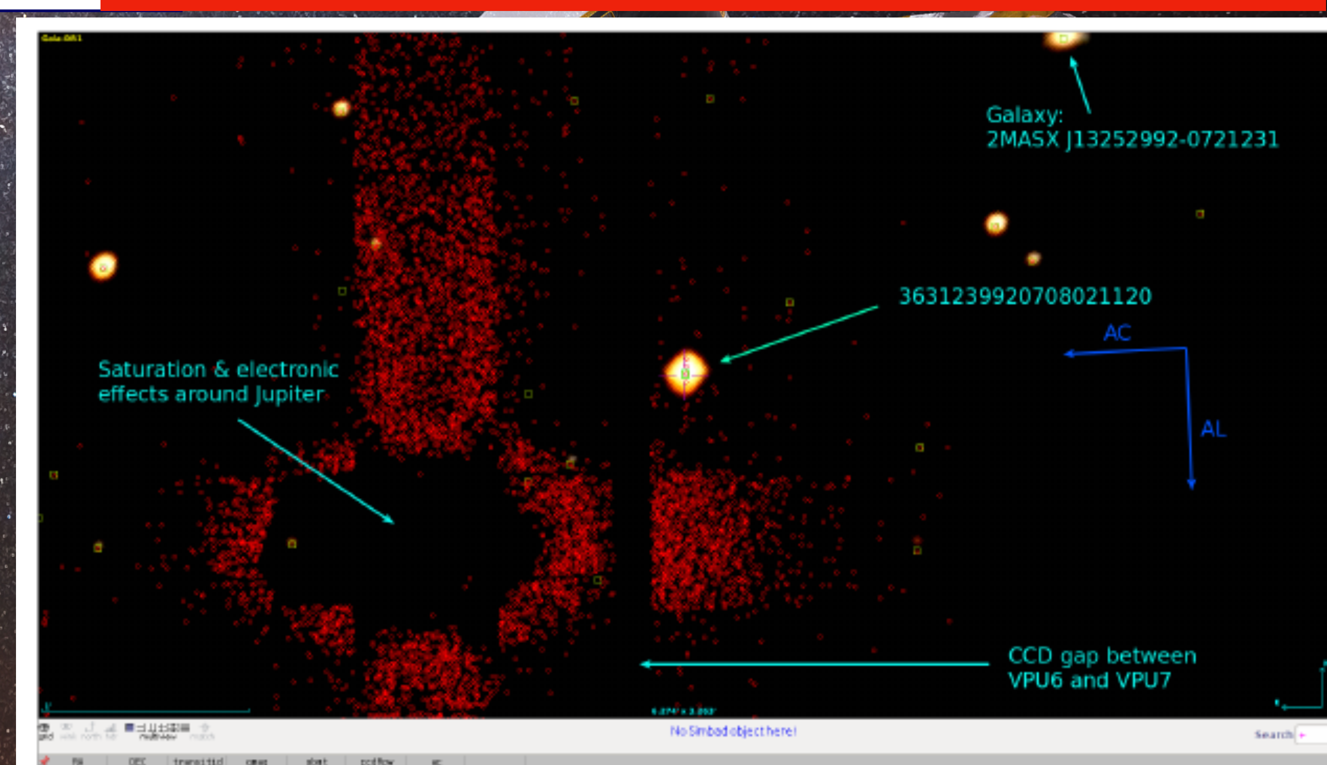

Observations for the **closest transit of the Target star** at an angular **separation of 6.73" from Jupiter's limb** seen on 2017-02-23T02:55:01.694

The Differential Astrometric measurements

Star field on different transits

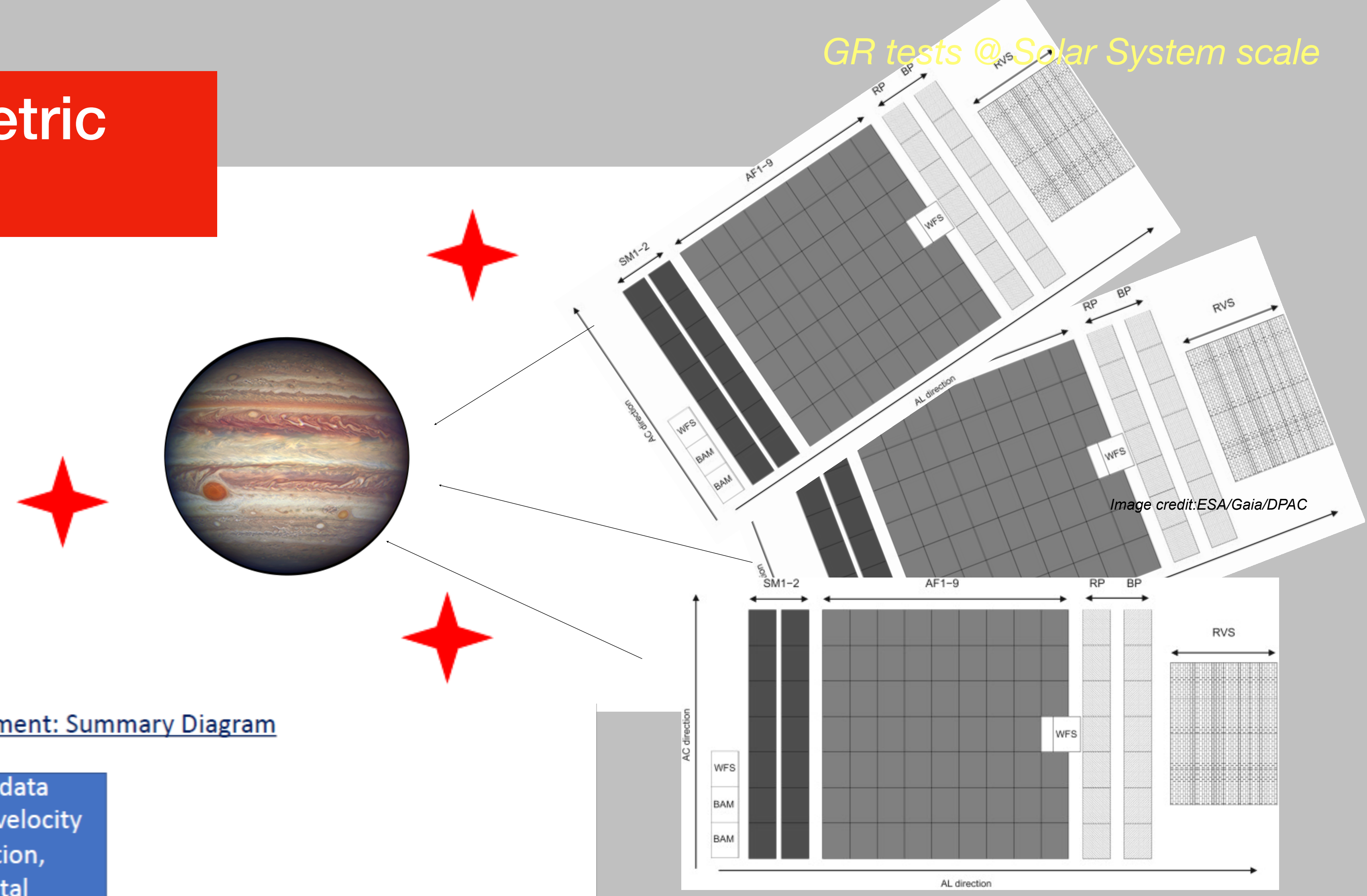

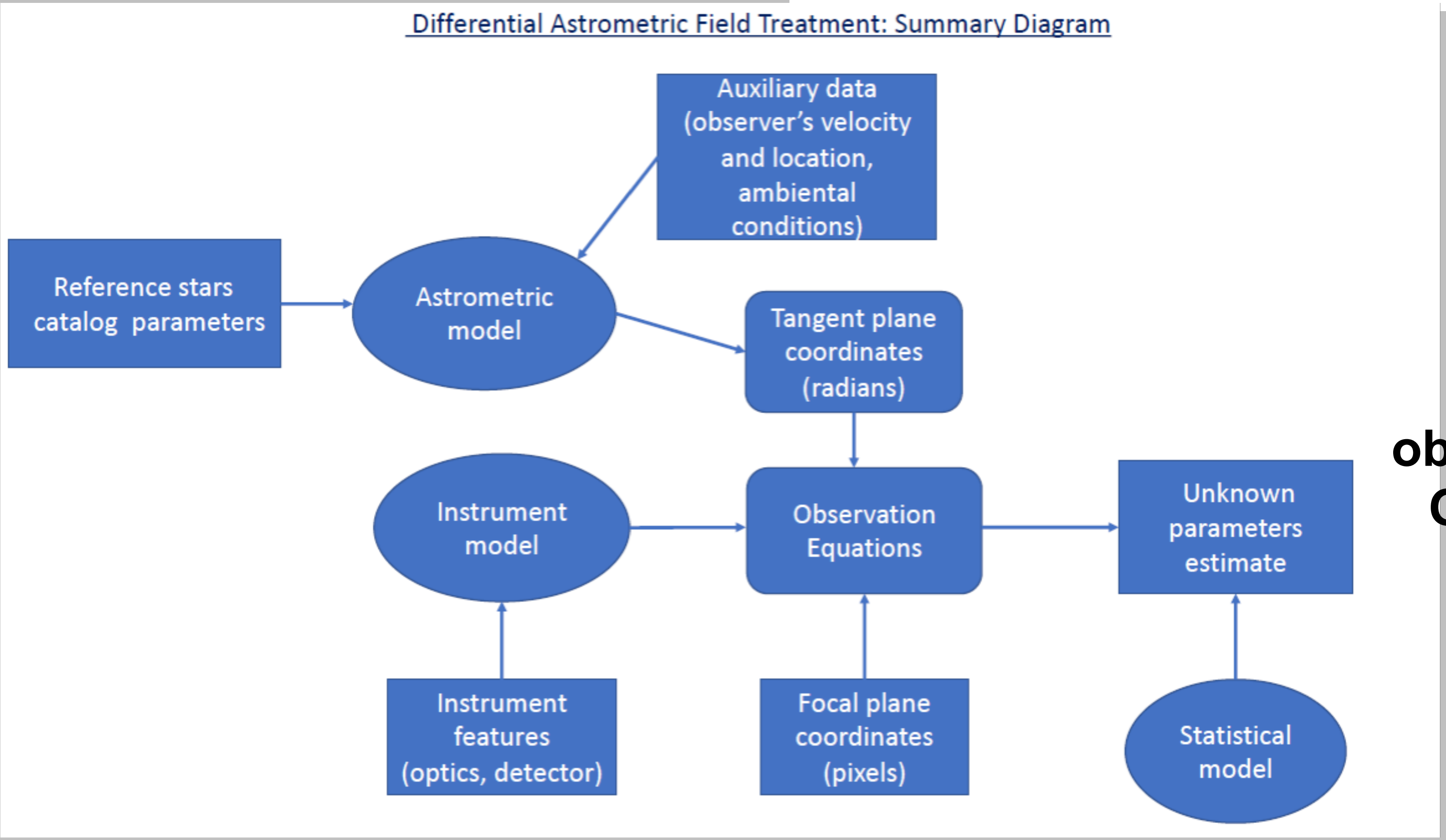

All differential astrometric analysis of the GAREQ observations developed at INAF-OATo supported by the Italian Gaia Data Proc. Center (@ ALTEC, To)

(Courtesy of B. Bucciarelli)

Compound Observations

- The same small fields are compared between close transits across the planet, avoiding the attitude error common to both transits

$$\Delta \mathbf{X} = \mathbf{x}(t_{i+1}) - \mathbf{x}(t_i)$$

TransitId	observed OBMT[long]	UTC	FOV	CCD row	b [Rjup]
1	104799283188665306	2017-02-22T19:08:02.862	1	7	4.29
2	104805682340958154	2017-02-22T20:54:42.015	2	7	3.61
3	104827296775979656	2017-02-23T02:54:56.450	2	6	1.35
4	104864126189227205	2017-02-23T13:08:45.862	1	2	2.85
5	104870525213255710	2017-02-23T14:55:24.887	2	3	3.55
6	104885740271535278	2017-02-23T19:08:59.945	1	2	5.24
7	104892139269141833	2017-02-23T20:55:38.943	2	3	5.96
8	104907354273083680	2017-02-24T01:09:13.947	1	1	7.67
9	104913753251905106	2017-02-24T02:55:52.925	2	2	8.40
10	104928968221338313	2017-02-24T07:09:27.895	1	1	10.14
11	104935367189558312	2017-02-24T08:56:06.863	2	2	10.88
12	104950582144816169	2017-02-24T13:09:41.818	1	1	12.64
13	104956981108577159	2017-02-24T14:56:20.782	2	2	13.38
14	104972196070729328	2017-02-24T19:09:55.744	1	1	15.17
15	104978595039079886	2017-02-24T20:56:34.713	2	2	15.92

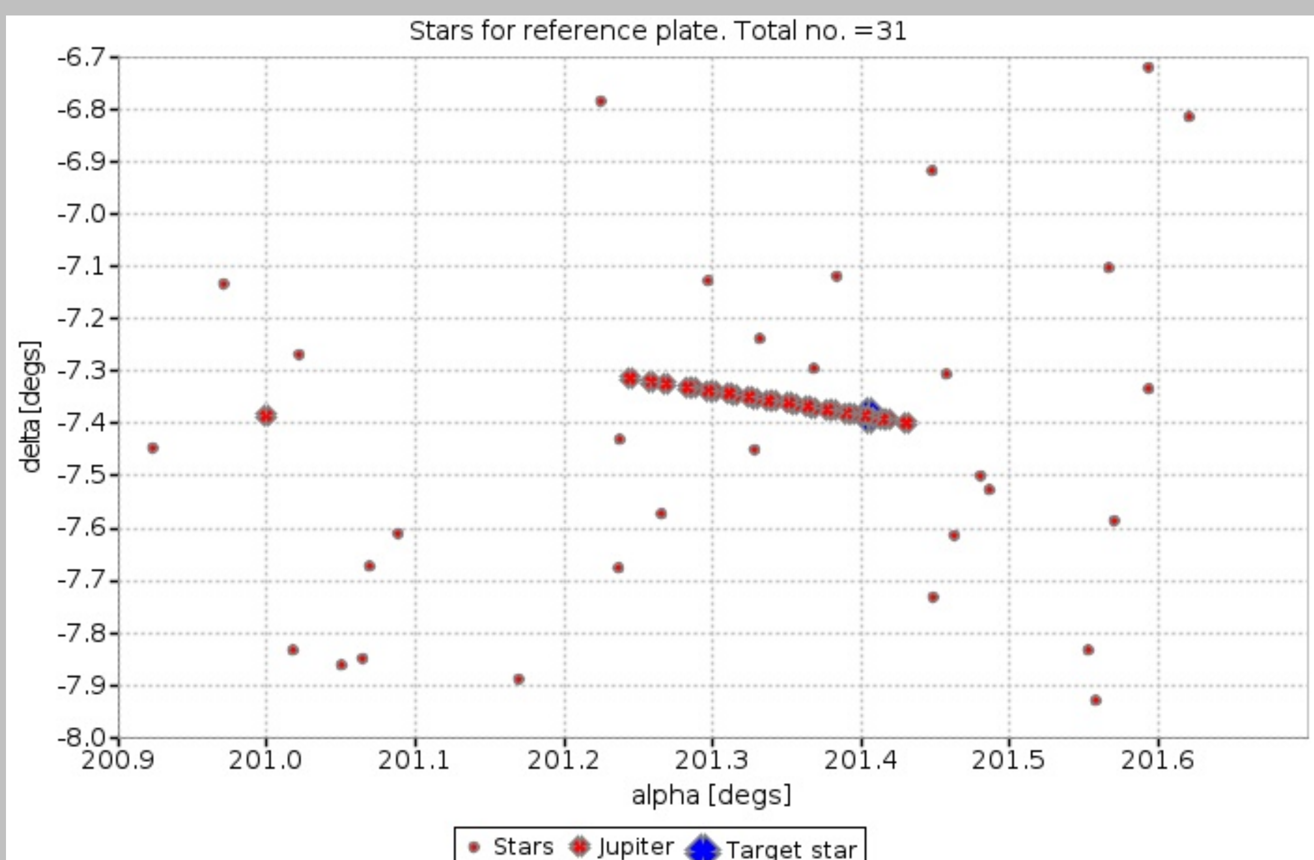

$$\Delta \boldsymbol{\Phi} = \Delta \Phi_1 \mathbf{n} + \Delta \Phi_2 \mathbf{m}$$

$$\Delta \Phi_1 = \frac{2(1+\gamma)M_p}{b_p}\left[1 + qJ_{2(p)}\frac{R_p^2}{b_p^2}\left(1 - 2(\mathbf{n}\cdot\mathbf{z})^2 - (\mathbf{t}\cdot\mathbf{z})^2\right)\right]$$

$$\Delta \Phi_2 = \frac{4(1+\gamma)M_p q J_{2(p)} R_p^2}{b^3}(\mathbf{m}\cdot\mathbf{z})(\mathbf{n}\cdot\mathbf{z})$$

- γ and q (*quadrupole efficiency factor*) are the only two unknowns of the model focus on the closest brightest star with G = 12.78 mag

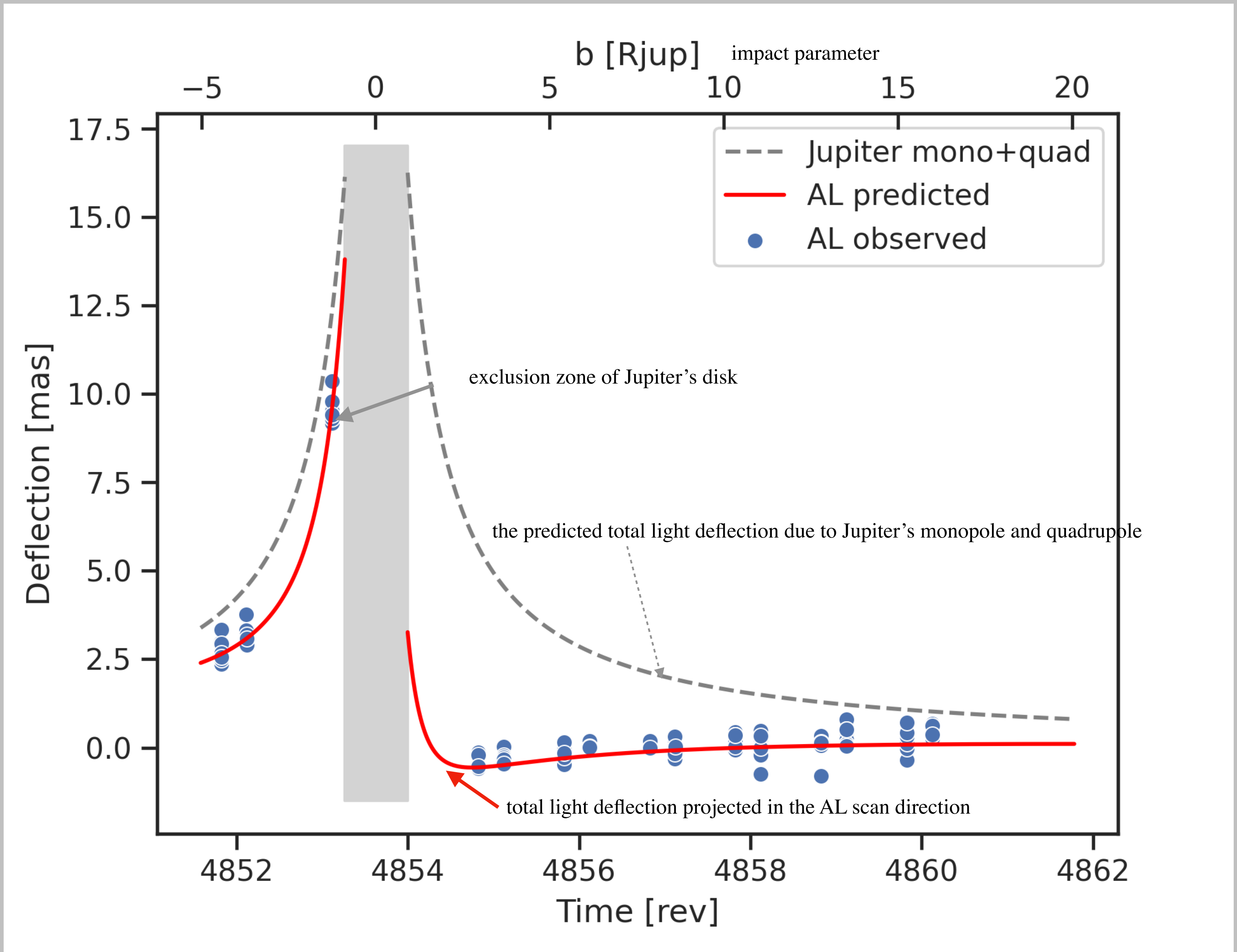

The AL coordinate for the target star at the various observing times plate-transformed to the reference frame calculated using the best-fit linear plate parameters per transit (OGA3).

(From Abbas, Bucciarelli, Lattanzi, Crosta, Busonero et al. , 2021, *Differential Astrometric analysis of the GAREQ experiment: Detection of the strongest Jupiter deflection signal with Gaia*)

(Details under ESA-DPAC Board review)

Compound shell observations

- The observable is the **relative stellar displacement** due to Jupiter's presence with respect to the zero-deflection position without Jupiter…Eddington rendition experiment!

$$\Delta R = r_{J+} - r_{J-}$$

Optimization on shell that enhances the quadrupole contribution -> technique suitable to detect very tiny relativistic effects, such as GW (POC2 activity within TLS experiment, The Living Sky, Premiale 2017)

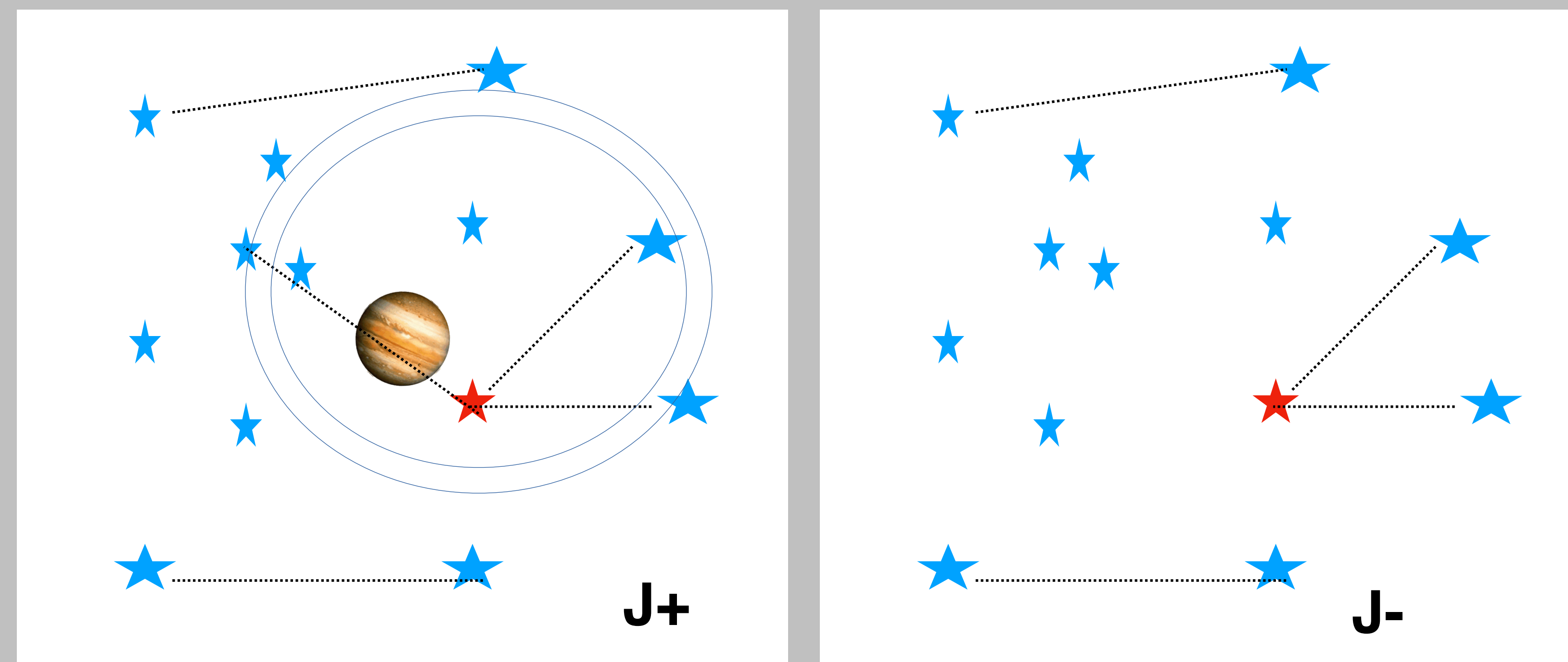

γ and ε with errors computed in the different formalism using simulated data

	Crosta and Mignard	LePoncin-Lafitte and Teyssandier	Kopeikin and Makarov	Erez-Rosen
$\gamma + \sigma_\gamma$	1.0001 ± 0.0037	1.0001 ± 0.0038	1.0000 ± 0.0036	0.9995 ± 0.0077
$q + \sigma_q$	0.9386 ± 0.8443	1.0844 ± 0.7925	1.0230 ± 0.2905	0.8753 ± 1.7627

	Crosta and Mignard	LePoncin-Lafitte and Teyssandier	Kopeikin and Makarov	Erez-Rosen
$\gamma + \sigma_\gamma$	0.9999 ± 0.0067	1.0000 ± 0.0067	1.0005 ± 0.0068	1.0013 ± 0.0153
$q + \sigma_q$	1.0104 ± 0.4035	1.0027 ± 0.3653	1.0256 ± 0.3375	1.1253 ± 1.8065

	Crosta and Mignard	LePoncin-Lafitte and Teyssandier	Kopeikin and Makarov	Erez-Rosen
$\gamma + \sigma_\gamma$	1.0000 ± 0.0001	1.0000 ± 0.0001	1.0000 ± 0.0036	0.9997 ± 0.0084
$q + \sigma_q$	1.0018 ± 0.0396	1.0012 ± 0.0379	1.0042 ± 0.0287	0.9623 ± 1.0926

- γ and q are the only two unknowns of the model

$$\mathbf{\Delta\Phi} = \Delta\Phi_1 \mathbf{n} + \Delta\Phi_2 \mathbf{m}$$

$$\Delta\Phi_1 = \frac{2(1+\gamma)M_p}{b_p}\left[1 + qJ_{2(p)}\frac{R_p^2}{b_p^2}\left(1 - 2(\mathbf{n}\cdot\mathbf{z})^2 - (\mathbf{t}\cdot\mathbf{z})^2\right)\right]$$

$$\Delta\Phi_2 = \frac{4(1+\gamma)M_p q J_{2(p)} R_p^2}{b^3}(\mathbf{m}\cdot\mathbf{z})(\mathbf{n}\cdot\mathbf{z})$$

From Crosta, Mignard (CQG, 2006)

Bini, Crosta, de Felice, Geralico,,Vecchiato. The Erez–Rosen metric and the role of the quadrupole on light propagation. Classical and Quantum Gravity, (4), 2013.
Crosta and Mignard. Microarcsecond light bending by Jupiter. Classical and Quantum Gravity, (15), 2006.
Kopeikin and Makarov. Gravitational bending of light by planetary multipoles and its measurement with microarcsecond astronomical interferometers. Phys. Rev. D, 75, Mar 2007.
Le Poncin-Lafitte and Teyssandier. Influence of mass multipole moments on the deflection of a light ray by an isolated axisymmetric body. Phys. Rev. D, 77, Mar 2008

from the observer to the star through space-time: the astrometric GW detection

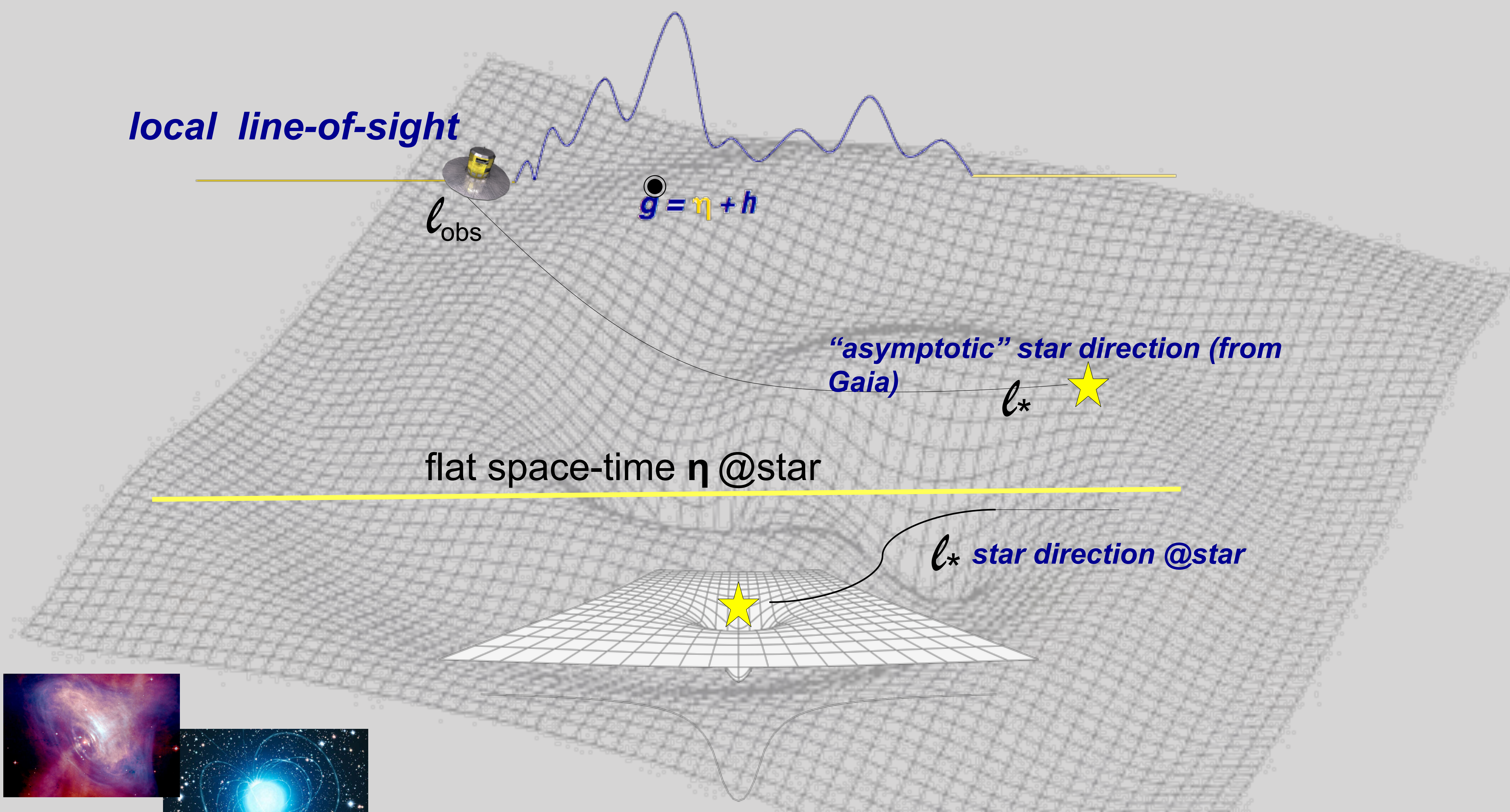

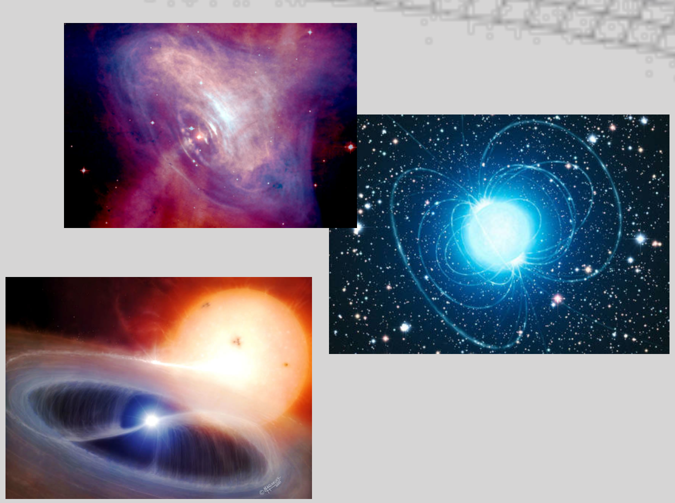

+ h_* @star

from the observer to the star through space-time: the astrometric GW detection

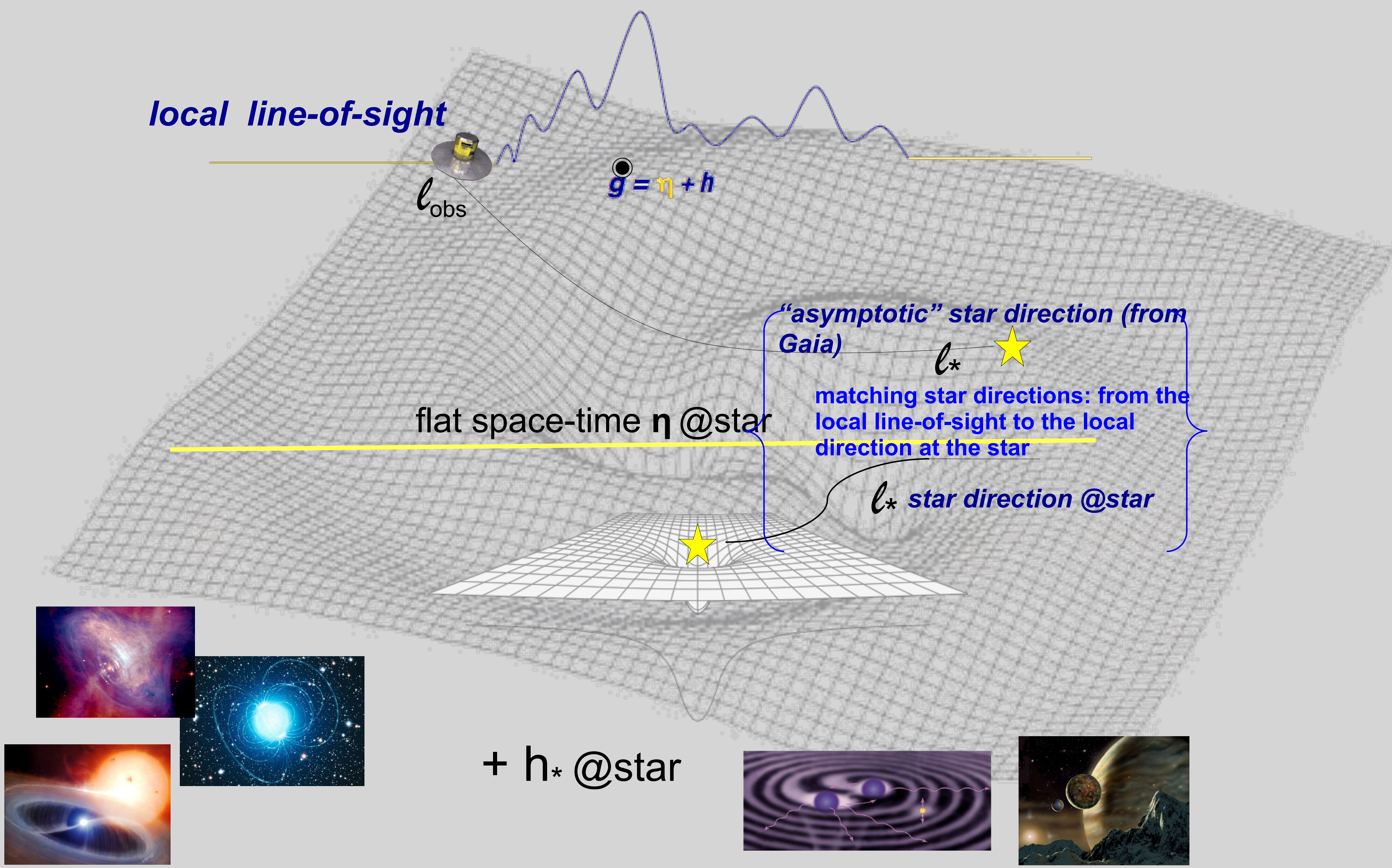

from the observer to the star through space-time: the astrometric GW detection

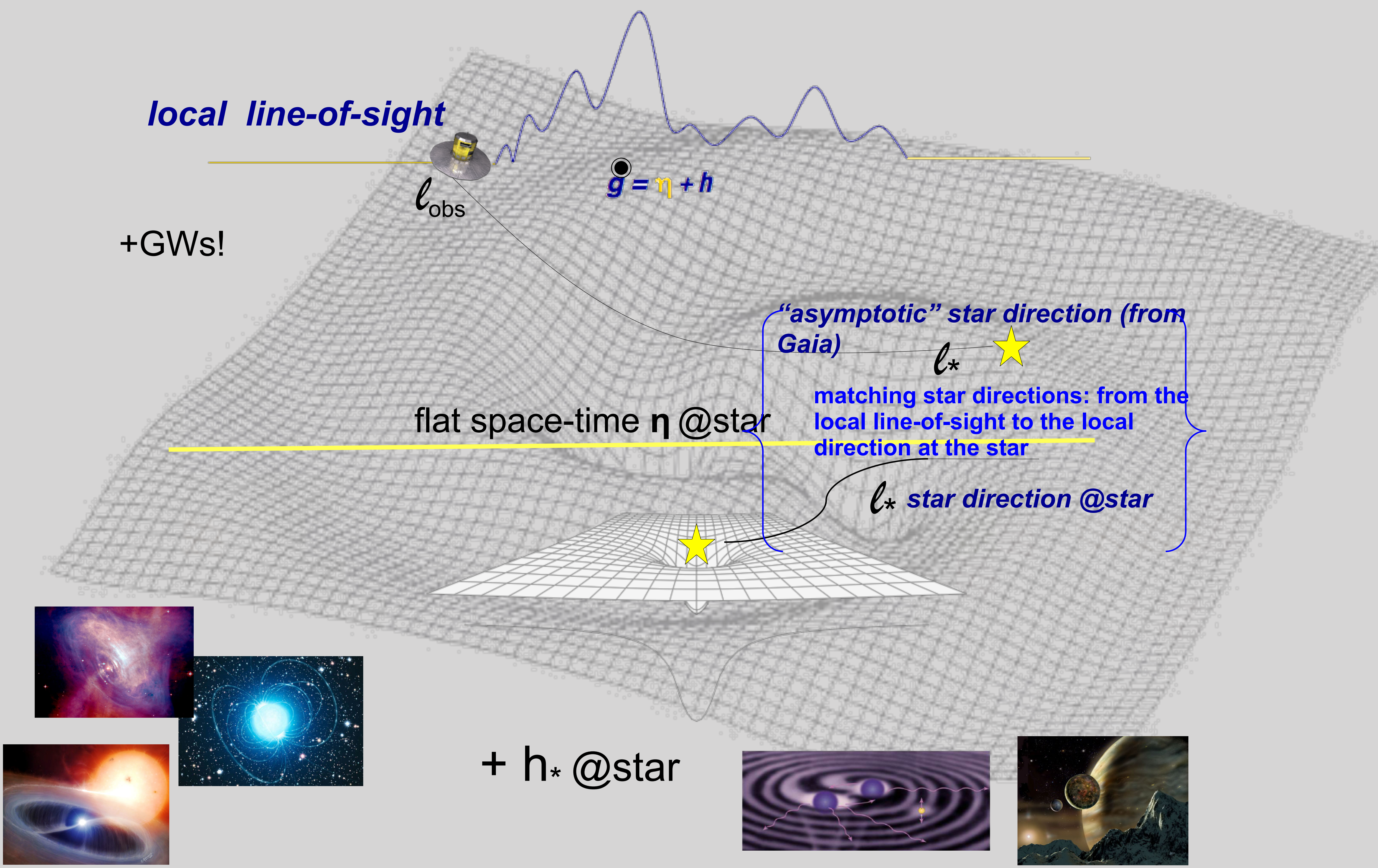

The fundamental observation equation for the astrometric GW antenna

$$\cos\psi_{1,2} = g_{\alpha\beta}(\bar{\ell}^{\alpha}_{1}\bar{\ell}^{\beta}_{2})_{obs} \,,$$

$$\bar{\ell}^{\alpha} = -\frac{\ell^{\alpha}}{(u\,|\,k)} = \bar{k}^{\alpha} - u^{\alpha}$$

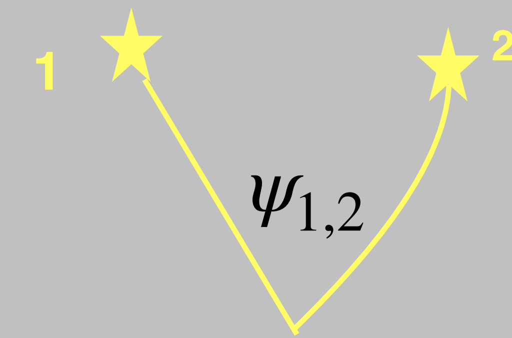

$$\cos\psi_{1,2} = \frac{P(u)_{\alpha\beta}k_1^{\alpha}k_2^{\beta}}{(\sqrt{P(u)_{\alpha\beta}k_1^{\alpha}k_1^{\beta}})(\sqrt{P(u)_{\alpha\beta}k_2^{\alpha}k_2^{\beta}})}$$

$$g_{\alpha\beta} = g^{SS}_{\alpha\beta} + h^{GW}_{\alpha\beta} = \eta_{\alpha\beta} + \sum_{(a)} h^{SS}_{(a)\alpha\beta} + h^{GW}_{\alpha\beta}$$

$$g_{\alpha\beta} = \eta_{\alpha\beta} + \boxed{\epsilon h^{SS}_{(1)\alpha\beta} + \epsilon^2 h^{SS}_{(2)\alpha\beta} + \epsilon^3 h^{SS}_{(3)\alpha\beta} + \epsilon^4 h^{SS}_{(4)\alpha\beta} + h^{GW}_{\alpha\beta} + O(\epsilon^5)} + O(h^2)$$

background metric with all terms at the same level of accuracy as the GWs in order to properly model all of the background systematic effect and disentagle the GW signals from such SS background (natural) "noises" ($\epsilon = v/c \sim 10^{-4}$rad -> $\epsilon^4 \sim$ narcsec

$$\bar{\ell}^{\alpha}_{obs} = \bar{\ell}^{\alpha(SS)} + \delta\ell^{\alpha(GW)} + O(\delta\ell^2)\,.$$

Similarly, stellar light directions can be separated into the SS part (due to the background metric) plus a perturbation shift, i.e. attributed purely to the passing GW

$$\bar{\ell}^{\alpha(SS)}_{obs} = \bar{\ell}^{\alpha}_{0} + \epsilon\bar{\ell}^{\alpha}_{(1)} + \epsilon^2\bar{\ell}^{\alpha}_{(2)} + \epsilon^3\bar{\ell}^{\alpha}_{(3)} + \epsilon^4\bar{\ell}^{\alpha}_{(4)} + O(\epsilon^5)\,.$$

$$\cos\psi_{1,2} = \cos\psi^{SS}_{1,2} + \underline{\eta_{\alpha\beta}(\bar{\ell}^{\alpha}_{1_0}\delta\ell^{\beta}_{2} + \bar{\ell}^{\alpha}_{2_0}\delta\ell^{\beta}_{1})_{obs} + h^{GW}_{\alpha\beta}\bar{\ell}^{\alpha}_{1_0}\bar{\ell}^{\beta}_{2_0}} + O(\epsilon^5) + O(h^2)$$

fundamental observation equation for the astrometric GW detection based on direction cosines relative to pairs of local line-of-sights

$$\boxed{F^{GW}_{1,2} \equiv \eta_{\alpha\beta}(\bar{\ell}^{\alpha}_{1_0}\delta\ell^{\beta}_{2} + \bar{\ell}^{\alpha}_{2_0}\delta\ell^{\beta}_{1})_{obs} + h^{GW}_{\alpha\beta}\bar{\ell}^{\alpha}_{1_0}\bar{\ell}^{\beta}_{2_0}}$$

$$\psi_{1,2} = \psi^{SS}_{1,2} + \delta\psi^{GW}_{1,2}$$

small perturbation due to the passing GW: $\delta\psi^{GW}_{1,2} \ll 1$

"large" angle from SS background

$$\boxed{\cos(\psi^{SS}_{1,2} + \delta\psi^{GW}_{1,2}) = \cancel{\cos(\psi^{SS}_{1,2})}\underbrace{\cos(\delta\psi^{GW}_{1,2})}_{\sim 1} - \sin(\psi^{SS}_{1,2})\underbrace{\sin(\delta\psi^{GW}_{1,2})}_{\sim \delta\psi} = \cancel{\cos\psi^{SS}_{1,2}} + F^{GW}_{1,2},}$$

$$\delta\psi^{GW}_{1,2} = -\frac{F^{GW}_{1,2}}{\sin(\psi^{SS}_{1,2})} + O(\epsilon^5) + O(h^2)$$

Crosta, Rivista del Nuovo Cimento 42, 10 (2019)

Crosta, Lattanzi, Leponcin-Lafitte, Gai, Zhaoxiang, Vecchiato , *On the principle of Astrometric Gravitational Wave Antenna, 2021 under review process*

In the far away zone, at L2 position

$$\delta\psi^{GW}_{1,2} = -\frac{h^{GW}_{ij(obs)}}{2\sin(\psi^{SS}_{1,2})}\left\{\frac{[\cos\psi_{1_0,2_0}+\cos\psi_{1_0,p}]\bar{\ell}^i_{2_0}\bar{\ell}^j_{2_0}}{(1+\cos\psi_{2_0,p})}+\frac{[\cos\psi_{1_0,2_0}+\cos\psi_{2_0,p}]\bar{\ell}^i_{1_0}\bar{\ell}^j_{1_0}}{(1+\cos\psi_{1_0,p})}\right\}$$

$$h_{ij} = A_{ij}\sin\omega(t-z)$$ Plane GW in TT gauge

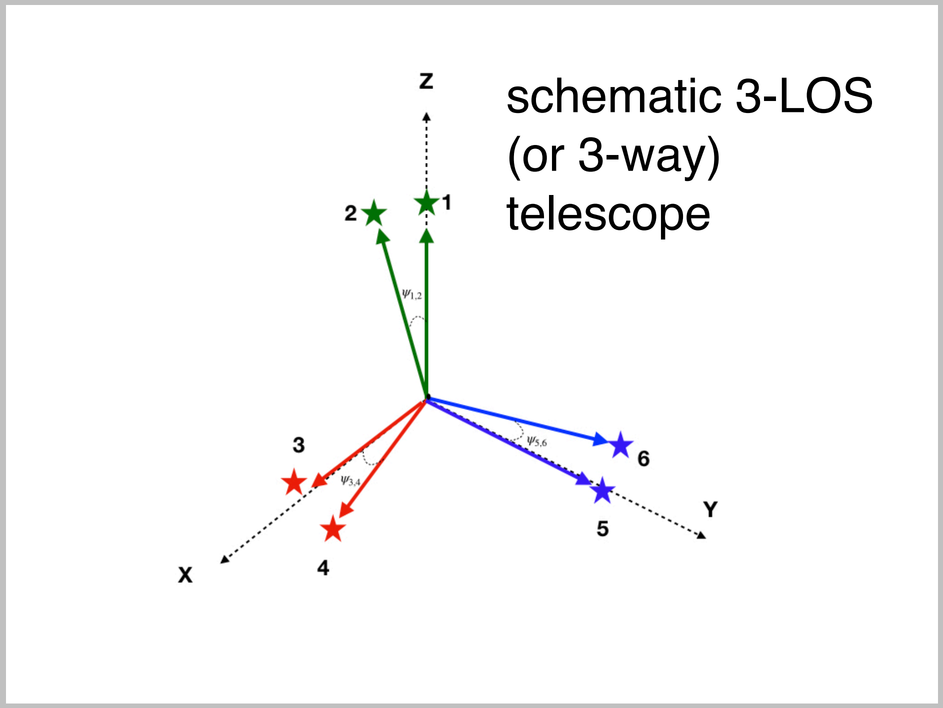

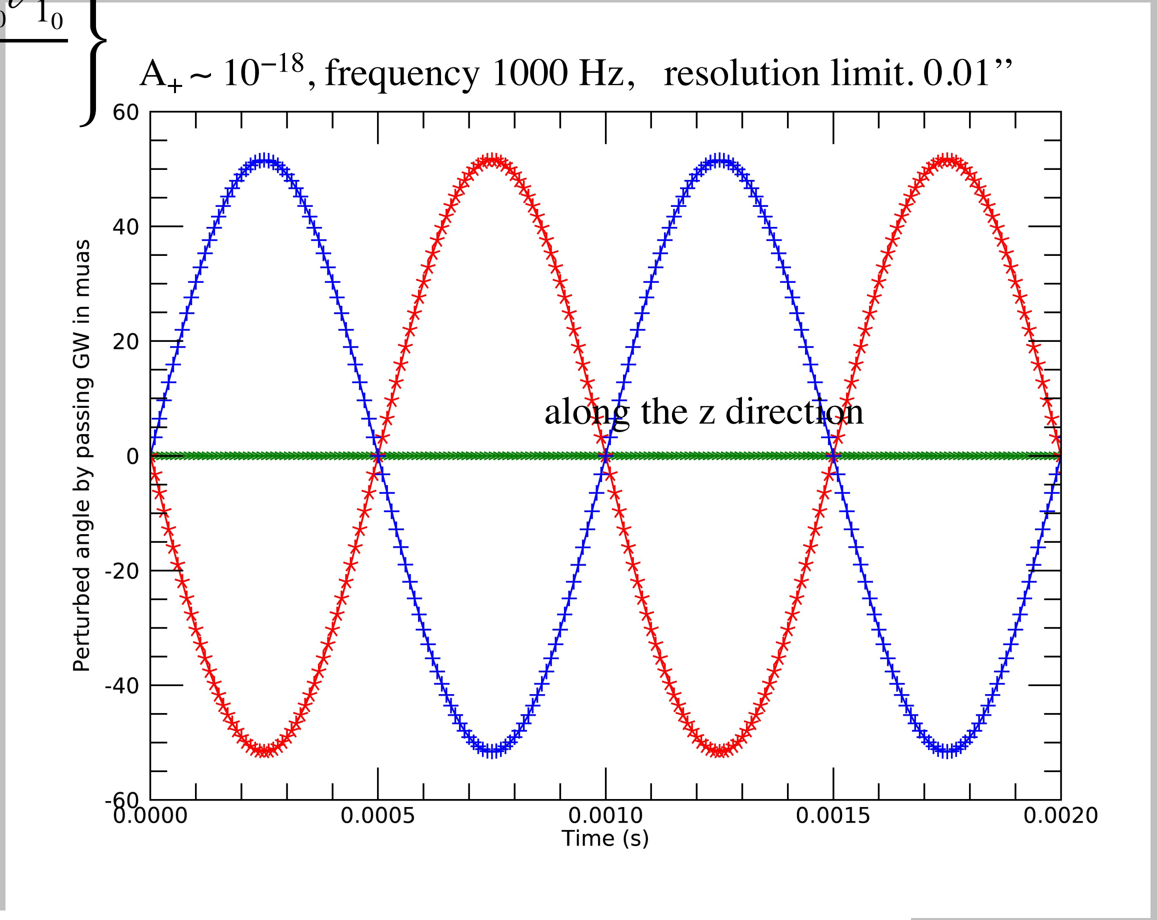

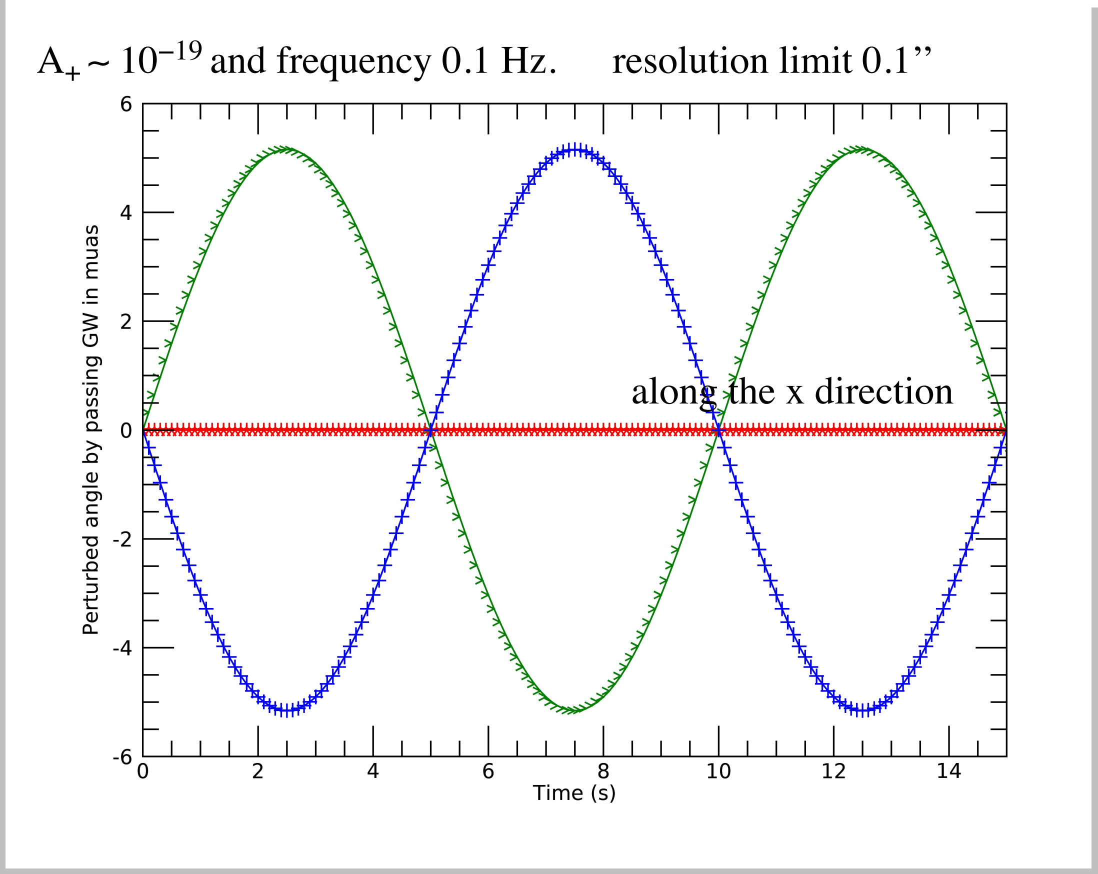

$max(\delta\psi^{GW}_{1,2})$ (μas)	$max(\delta\psi^{GW}_{3,4})$ (μas)	$max(\delta\psi^{GW}_{5,6})$ (μas)	A_+ (radians)	ψ_{i_0,j_0} (”)
4.12×10^{-15}	5.12	5.12	10^{-18}	0.1
4.12×10^{-16}	0.51	0.52	10^{-19}	0.1
4.12×10^{-17}	5.12×10^{-2}	5.12×10^{-2}	10^{-20}	0.1
0	5.12×10^{-3}	5.12×10^{-3}	10^{-21}	0.1
4.12×10^{-16}	51.57	51.57	10^{-18}	0.01

Amplitude of the angular perturbations for different linear strains of amplitude A_+ (radians) propagating along the $e_z$direction

Perspectives for the GW astrometric detection

★ Advantages in using close pairs of stars, e.g.:

- mitigation of high perturbative terms and amplification of the GW signal
- exploit a large number of null geodesics, so that **to scrutinize the GW direction;**
- avoid the satellite's attitude
- GW astrometric observation equation accounting for a wide range of frequencies;
- link the properties of a GW source with extensive statistics;
- pave the way for new GW tests on the graviton interaction with photon;
- enable tests on GW polarization modes by combining different telescope orientations

★ 0.01" resolution is already available with operating telescopes (HST and Gaia), or that will soon operate in space (**Lattanzi's talk!**)

★ Use of the DPCT archives astroelementary measurements, i.e. each stellar transit on astrometric/ photometric CCD row. Since Gaia is mapping continuously the sky down to the G=21 this would help to determine in the visible band distance to the GWs source if it happens to be observed in one of the Gaia FOVs. A protocol (i.e. software to analyse residuals in the source parameters such as centroid shift, flux variation, etc..) for a quick response to this kind of signal is going to be implemented at DPCT.

- Possibly a differential procedure similar to that of GAREQ can be used to single out GWs effects - if measurable - on a stellar fields i.e. shift on the light proper direction as observed by Gaia before and after the GWs detection.
- Future work (in collaboration also with Oa Cagliari and UNiv. Bicocca/Insubria, PRIN "Push gravity frontiers", PI Sesana) will focus on possible synergies with PTA, modeling this signal in prospective to spot specific GW galactic candidates and improve the probing of the Gw waves sources (including primordial GW) -> likely beyond Gaia!

Lesson from Gaia

- Any GR tests performed by using Gaia @SS or @MW scale can play a reference role for other tests, much like the Sun for the stars, the Earth/Jupiter for exoplanets, our Galaxy for other galaxies, non-spherical weak lensing and so on..
- The mandatory use of GR has opened new possibilities and strategies to apply Einstein's Theory in classical astronomy domain, providing new coherent methods and "laboratories" to exploit at best the standard theory of gravity
- The first results are really promising (a fully 4D relativistic sky, MW rotation curve, GW astrometric antenna to scrutinize GW directions and maybe more to come..) and push towards more complicate solutions (i.e. a relativistic Galaxy model, local cosmology tests..)

Lesson from Gaia

- Any GR tests performed by using Gaia @SS or @MW scale can play a reference role for other tests, much like the Sun for the stars, the Earth/Jupiter for exoplanets, our Galaxy for other galaxies, non-spherical weak lensing and so on..
- The mandatory use of GR has opened new possibilities and strategies to apply Einstein's Theory in classical astronomy domain, providing new coherent methods and "laboratories" to exploit at best the standard theory of gravity
- The first results are really promising (a fully 4D relativistic sky, MW rotation curve, GW astrometric antenna to scrutinize GW directions and maybe more to come..) and push towards more complicate solutions (i.e. a relativistic Galaxy model, local cosmology tests..)

Thank you very much for your attention!